NACA RM A9L27

RESEARCH MEMORANDUM

HIGH-SPEED AERODYNAMIC CHARACTERISTICS OF A LATERAL-CONTROL MODEL. II - MODIFIED NACA 0012-64 SECTION WITH A 26.6-PERCENT-CHORD, PLAIN, TRAILING-EDGE AILERON; WING UNSWEPT AND SWEPT BACK 45°

By Walter J. Krumm and Joseph L. Anderson

Ames Aeronautical Laboratory
Moffett Field, Calif.

NATIONAL ADVISORY COMMITTEE
FOR AERONAUTICS

WASHINGTON
March 15, 1950

NATIONAL ADVISORY COMMITTEE FOR AERONAUTICS

RESEARCH MEMORANDUM

HIGH-SPEED AERODYNAMIC CHARACTERISTICS OF A LATERAL-CONTROL MODEL. II - MODIFIED NACA 0012-64 SECTION WITH A 26.6-PERCENT-CHORD, PLAIN, TRAILING-EDGE AILERON; WING UNSWEPT AND SWEPT BACK 45°

By Walter J. Krumm and Joseph L. Anderson

SUMMARY

In order to obtain lateral-control information for use in the design of aircraft, wind-tunnel tests were made to determine the aerodynamic characteristics of a semispan wing with a modified NACA 0012-64 section and a 26.6-percent-chord, plain, trailing-edge aileron. Results are shown for the wing with the 0.229-chord line unswept and swept back 45° and for a Mach number range from 0.40 to 0.925. Data were obtained with the trailing-edge aileron deflected from 0° to 15°.

The results for the unswept wing showed that the onset of trailing-edge aileron overbalance and loss in effectiveness did not occur until approximately the Mach number of lift and drag divergence was reached. The results for the wing swept back showed that the aileron did not overbalance or lose effectiveness up to the highest test Mach number (0.925).

INTRODUCTION

As a basis for the development of methods for adequate lateral control of high-speed airplanes, an investigation was undertaken in the Ames 16-foot high-speed wind tunnel of a lateral-control-development model. This model consisted of a semispan wing with an NACA 0012-64 section fitted with a 20-percent-chord, plain, trailing-edge aileron. (See reference 1.) Early in the investigation it was found that the aileron became overbalanced and lost effectiveness at moderate speeds and was therefore not suitable for a general study. The trailing-edge angle was reduced from 20.6° to 13.1° by extending the trailing edge 9 percent of the wing chord in order to delay this overbalance and loss in effectiveness.

The test results presented in this report are for the semispan wing with the modified NACA 0012-64 section and with a 26.6-percent-chord, plain, trailing-edge aileron.

NOTATION

The coefficients and symbols used in this report are defined as follows:

C_D drag coefficient $\left(\frac{\text{drag}}{qS}\right)$

C_{h_a} aileron hinge-moment coefficient $\left(\frac{\text{aileron hinge moment}}{q\,\overline{c_a}^2\,b_a}\right)$

C_L lift coefficient $\left(\frac{\text{lift}}{qS}\right)$

C_l rolling-moment coefficient about a longitudinal axis at the root chord parallel to the air stream $\left(\frac{\text{rolling moment}}{4qSb}\right)$

C_m pitching-moment coefficient about a lateral axis passing through the quarter point of the mean aerodynamic chord $\left(\frac{\text{pitching moment}}{qS\overline{c}}\right)$

C_{L_δ} $\left(\frac{\partial C_L}{\partial \delta_a}\right)_{\alpha=0^\circ}$

C_{l_δ} $\left(\frac{\partial C_l}{\partial \delta_a}\right)_{\alpha=0^\circ}$

C_{m_δ} $\left(\frac{\partial C_m}{\partial \delta_a}\right)_{\alpha=0^\circ}$

A aspect ratio $\left(\frac{2b^2}{S}\right)$

a speed of sound in air, feet per second

b semispan of model, feet

b_a aileron span parallel to the hinge line, feet

c chord of the wing parallel to the plane of symmetry, feet

$\bar{c}$ mean aerodynamic chord $\left(\frac{\int_0^b c^2 dy}{\int_0^b c\, dy}\right)$, feet

$\overline{c_a}$ root-mean-square chord of aileron between hinge line and the free edge measured perpendicular to the hinge line, feet

M Mach number $\left(\frac{V}{a}\right)$

q dynamic pressure $\left(\frac{\rho V^2}{2}\right)$, pounds per square foot

R Reynolds number $\left(\frac{\rho V \bar{c}}{\mu}\right)$

S area of semispan model, square feet

V velocity of the free air stream, feet per second

y spanwise distance from wing root, feet

α angle of attack of model, degrees

Δ increment due to aileron deflection

δ_a aileron deflection measured in a plane normal to the hinge line, positive when the free edge is deflected downward, degrees

μ absolute viscosity of air in the free air stream, pound-seconds per square foot

ρ mass density of air in the free air stream, slugs per cubic foot

The subscripts used denote the following:

u uncorrected

L.E. leading edge

T.E. trailing edge

DESCRIPTION OF MODEL AND APPARATUS

The model was a semispan wing with the NACA 0012-64 section perpendicular to the 0.25-wing-chord line as used in reference 1, but was modified for these tests by extending the trailing edge 9 percent of the wing chord. This afterportion was developed by drawing straight lines tangent to the section and to the trailing-edge radius. This modification changed the reference-chord line from the 0.25-chord line to the 0.229-chord line. The coordinates for this modified section, which was 11 percent thick, are given in table I. This modification reduced the trailing-edge angle from 20.6° to 13.1°.

Tests of the model both unswept and swept back 45° were conducted in the Ames 16-foot high-speed wind tunnel. The wing spar of the model extended through the tunnel wall and fastened to the balance frame. For the wing unswept the 0.229-chord line was perpendicular to the air stream. For the wing swept back 45° the model was rotated back about the 0.459-root-chord point until the 0.229-chord line was 45° to the air stream. Model geometry for the wing unswept and swept back 45° is listed in table II and is shown in figure 1. A baffle (fig. 2) was installed on the model near the tunnel wall to direct the leakage air from the tunnel-wall gap away from the surface of the model.

The wing was fitted with a leading-edge aileron and a trailing-edge aileron. The leading-edge aileron was installed as is indicated in figure 1, but was not deflected for the tests reported here. The trailing-edge aileron occupied 26.6 percent of the wing chord perpendicular to the 0.229-chord line and extended from 0.56 of the unswept-wing semispan to the tip and extended from 0.48 of the swept-back-wing semispan to the tip. This aileron was flat-sided with a radius nose and was also unsealed. For these tests this aileron was deflected from 0° to 15°. There were gaps of 1/16 inch between the ailerons and the wing. The aileron was restrained by a cantilever beam to which were glued resistance-type strain gages for the measurement of the hinge moments.

The tunnel test section was modified between the tests of reference 1 and the tests of this report. This tunnel modification was made by the addition of flats to the tunnel walls which reduced the test-section breadth to 12 feet.

CORRECTIONS TO DATA

The test Mach numbers were corrected for the blockage effect of the model by the method outlined in reference 2. This correction increased the uncorrected Mach number about 1 percent at 0.80 Mach number and about 4 percent at 0.925 Mach number. The angle of attack, the drag coefficients, and the rolling-moment coefficients were corrected for the effects of the tunnel walls by the method outlined in reference 3. These corrections differ from those of reference 1 because of the change in the size of the tunnel test section after the tests of reference 1. The span load distributions for a Mach number of 0.80, as determined from static pressure measurements, were used as a basis for these corrections.

The corrections were applied to the data as follows:

For the wing unswept:

$$\alpha = \alpha_u + 0.621C_L$$

$$C_D = C_{D_u} + 0.0094C_L^2$$

$$C_l = 0.894C_{l_u}$$

For the wing swept back 45°:

$$\alpha = \alpha_u + 0.619C_L$$

$$C_D = C_{D_u} + 0.0090C_L^2$$

$$C_l = 0.892C_{l_u}$$

No corrections were made for the effect of the approximately 3-inch-thick tunnel-wall boundary layer passing over the model. No corrections were made for the effects of elastic deformation of the aileron or wing under load as the rigidity of the model made these corrections negligible.

RESULTS AND DISCUSSION

The results presented in this report are for the semispan wing unswept and swept back 45° for a Mach number range from 0.40 to 0.925, and with the trailing-edge aileron deflected from 0° to 15°. The average Reynolds numbers for these tests are shown in figure 3.

The aerodynamic characteristics for the wing unswept and swept back 45° and with the control surfaces undeflected are shown in figures 4 through 6. Figure 4 shows the variation of lift coefficient with angle of attack; figure 5 shows the variation of drag coefficient with Mach number; and figure 6 shows the variation of pitching-moment coefficient with lift coefficient. The Mach number of lift and drag divergence for the wing unswept was about 0.82 at low lift coefficients. For the wing swept back 45°, the lift and drag divergence had not been reached at the highest Mach number of the tests (0.925).

The results of the tuft studies of the flow over the wing unswept and swept back 45° are shown in figures 7 and 8. For the wing unswept, the flow separated first in the region of the inboard end of the trailing-edge aileron and the separation progressively covered a larger area as the stall was approached. The surface discontinuities caused by the clearance gaps at the inboard ends of both ailerons probably contributed to the separation in this area. For the wing swept back 45°, the flow of air began to separate first at the wing tip and, as the angle of attack was increased, the separation progressively covered a larger area. For both the wing unswept and swept back 45°, the flow of air over the wing root was parallel to the tunnel wall and showed no indication of disturbance by the gap at the tunnel wall.

The increments of rolling-moment coefficient due to deflection of the trailing-edge aileron for the wing unswept and swept back 45° are shown in figure 9. The increment of rolling-moment coefficient was obtained by the transfer of the rolling moment about the balance axis to the model axis and the subtraction of the rolling moment due to the wing itself. This resulted in some scatter; therefore, the rolling-moment coefficients were faired to obtain the data as presented. The variations

of the effectiveness parameters C_{L_δ}, C_{m_δ}, and C_{l_δ} of the trailing-edge aileron with Mach number are shown in figure 10. A positive aileron deflection produced a negative increment of rolling-moment coefficient (fig. 9(a)) at 0.875 Mach number and -4° angle of attack, and at 0.90 Mach number and -4°, -2°, and 0° angle of attack. Figure 10 shows that, for the unswept wing, the aileron effectiveness C_{l_δ} increased slightly with increase in Mach number up to a Mach number of 0.77 (about the Mach number of divergence). Before the trailing edge was modified (reference 1), the aileron decreased in effectiveness with increase in Mach number above a Mach number of 0.60. For the wing swept back 45° (fig. 9(b)), there was a greater decrease in increment of rolling-moment coefficient for the trailing-edge aileron with increase in angle of attack at 0.40 Mach number than at higher Mach numbers. The parameters C_{L_δ}, C_{m_δ}, and C_{l_δ} are shown to diverge at about the same Mach number (fig. 10). The Mach number of divergence, with the wing unswept, occurred at about 0.80 Mach number for each parameter, while the Mach number of divergence is not clearly defined for the swept wing.

The hinge-moment coefficients for the trailing-edge aileron for the wing unswept and swept back 45° are shown in figures 11 and 12. For the wing unswept, the Mach number at which overbalance occurred for the trailing-edge aileron was about 0.85 (fig. 11). This was an increase of about 0.15 Mach number over that Mach number at which overbalance of the trailing-edge aileron occurred before the trailing edge of the wing was modified (reference 1). Reducing the trailing-edge angle from 20.6° to 13.1° by the trailing-edge modification probably accounted for the major part of this increase, with the reduction in wing thickness making some contribution. For the wing swept back, the trailing-edge aileron never became overbalanced at or below the highest test Mach number (0.925).

CONCLUDING REMARKS

From the tests of the lateral-control-development model with a modified NACA 0012-64 section it was found that, with a trailing-edge angle of about 13°, the trailing-edge aileron remained effective and did not become overbalanced on the unswept wing up to at least the Mach number of lift and drag divergence of the wing. With the wing swept back 45°, this trailing-edge aileron remained effective and did not become overbalanced up to the maximum Mach number of the tests (0.925).

Ames Aeronautical Laboratory,
National Advisory Committee for Aeronautics,
Moffett Field, California.

REFERENCES

1. Anderson, Joseph L., and Krumm, Walter J.: High-Speed Aerodynamic Characteristics of a Lateral-Control Model. I - NACA 0012-64 Section with 20-Percent-Chord Plain Aileron and 0° and 45° Sweepback. NACA RM A8H12, 1948.

2. Herriot, John G.: Blockage Corrections for Three-Dimensional-Flow Closed-Throat Wind Tunnels, with Consideration of the Effects of Compressibility. NACA RM A7B28, 1947.

3. Swanson, Robert S., and Toll, Thomas A.: Jet-Boundary Corrections for Reflection-Plane Models in Rectangular Wind Tunnels. NACA Rep. 770, 1943.

TABLE I.- COORDINATES IN PERCENT CHORD

FOR THE MODIFIED NACA 0012-64 SECTION

Station	Ordinate
0	0
1.25	1.80
2.50	2.40
5.00	3.12
7.50	3.62
10.00	4.01
15.00	4.58
20.00	4.98
25.00	5.25
30.00	5.41
35.00	5.50
40.00	5.48
45.00	5.37
50.00	5.18
55.00	4.88
60.00	4.50
70.00	3.45
80.00	2.32
90.00	1.21
100.00	0
L.E. radius:	1.45
T.E. radius:	.10

TABLE II.- MODEL DIMENSIONS

Dimension	Unswept wing	Swept-back wing
Semispan, feet	7	5.327
Semispan area, square feet	13.3	13.17
Aspect ratio (based on full span)	7.37	4.31
Taper ratio	0.50	0.48
Mean aerodynamic chord, feet	2.01	2.68
Distance from root chord to mean aerodynamic chord, feet	3.05	2.27
Wing root chord parallel to the air stream, feet	2.572	3.442
Projected tip chord parallel to the air stream, feet	1.286	1.657
Sweep of leading edge, degrees	2.41 back	47.41 back
Sweep of 0.229 wing-chord line, degrees	0	45 back
Sweep of trailing edge, degrees	8.06 forward	36.94 back
Sweep of leading-edge aileron hinge line, degrees	0.95 back	45.95 back
Sweep of trailing-edge aileron hinge line, degrees	5.30 forward	40.60 back
Wing thickness, based on chord parallel to the air stream, percent chord	11.01	8.39
Trailing-edge angle, in plane parallel to the air stream, degrees	13.12	10.0

TABLE II.- Concluded

Dimension	Unswept wing	Swept-back wing
Section, perpendicular to the 0.229-wing-chord line (see table I)	NACA 0012-64 modified by extending the trailing-edge 9-percent chord	
Trailing-edge aileron:		
Ratio of aileron chord to wing chord, perpendicular to the 0.229-wing-chord line	0.2660	
Span along the hinge line, feet	3.070	
Root-mean-square chord, feet	0.407	
Area, behind hinge line, square feet	1.136	

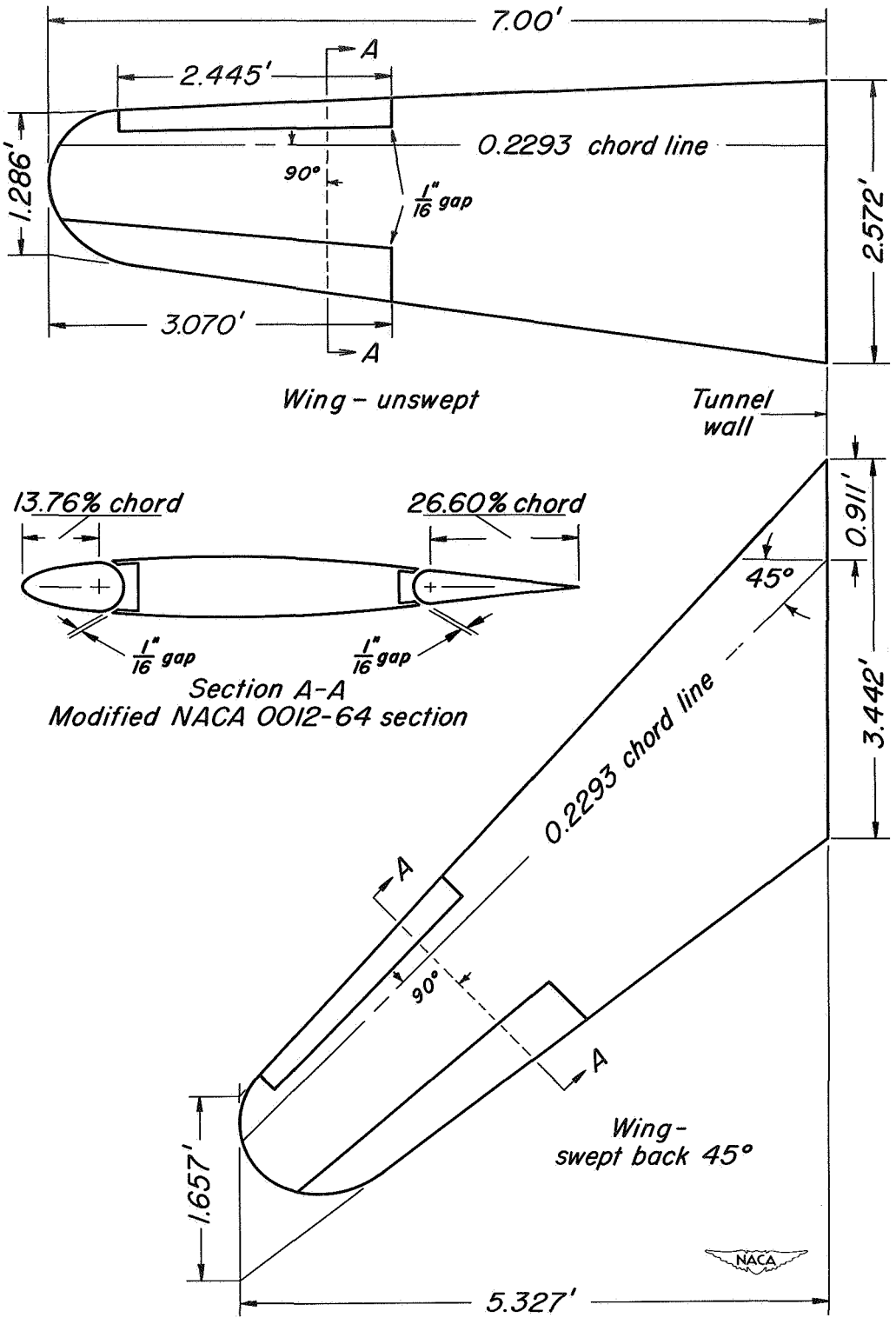

Figure 1.- Geometry of the lateral-control-development model.

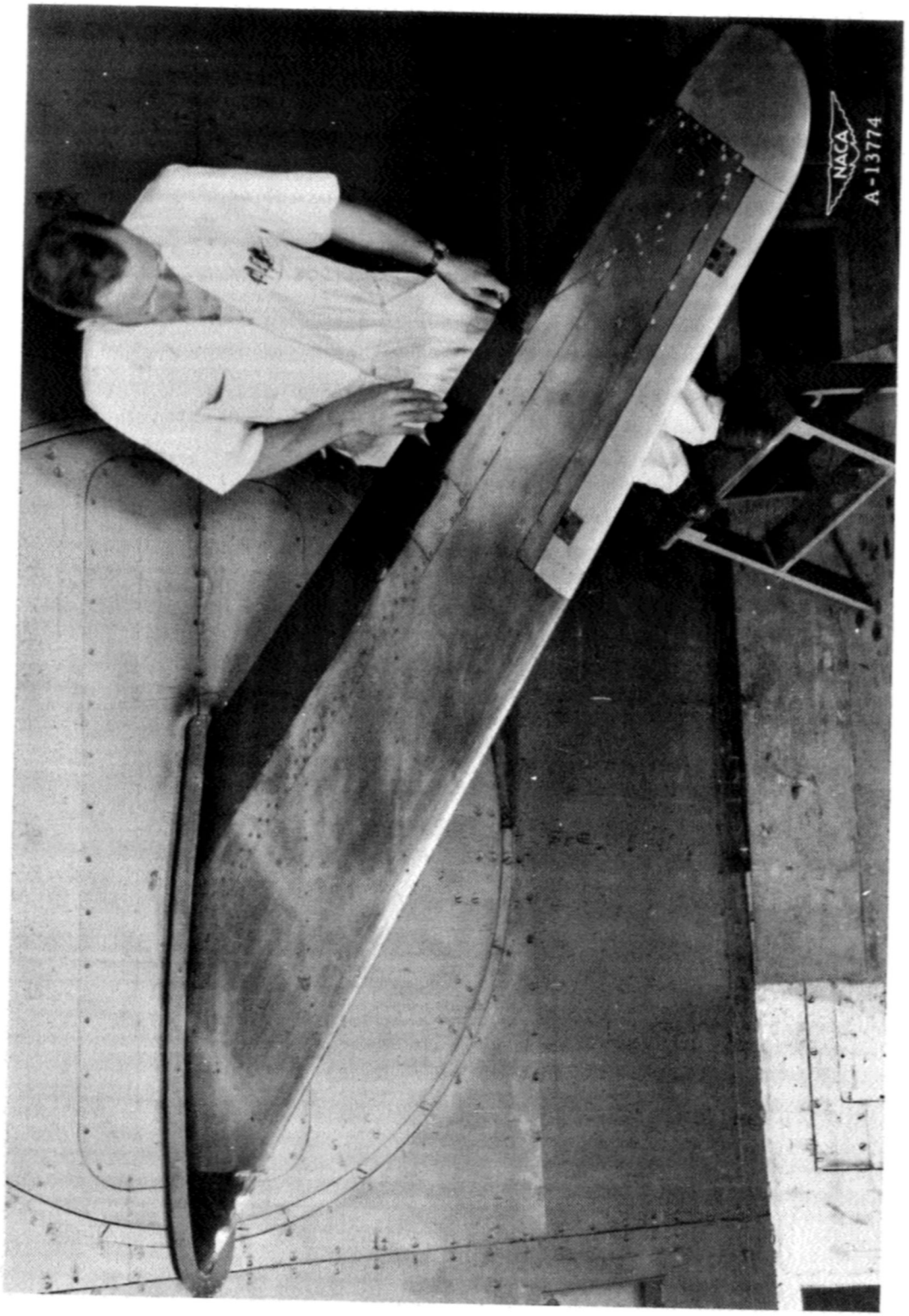

Figure 2.- Model mounting arrangement, wing swept back 45°.

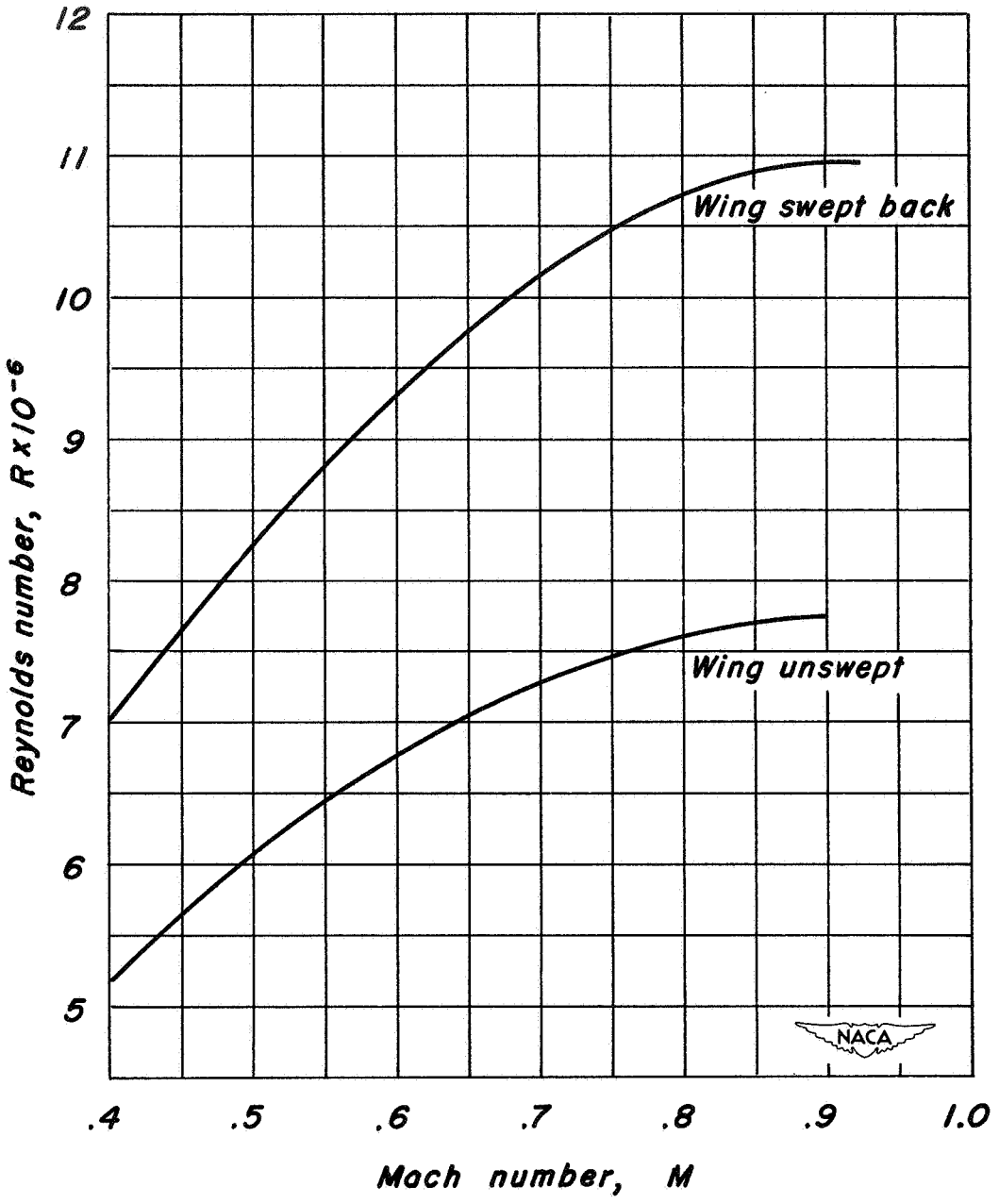

Figure 3.- Variation of Reynolds number with Mach number for the wing unswept and swept back 45°.

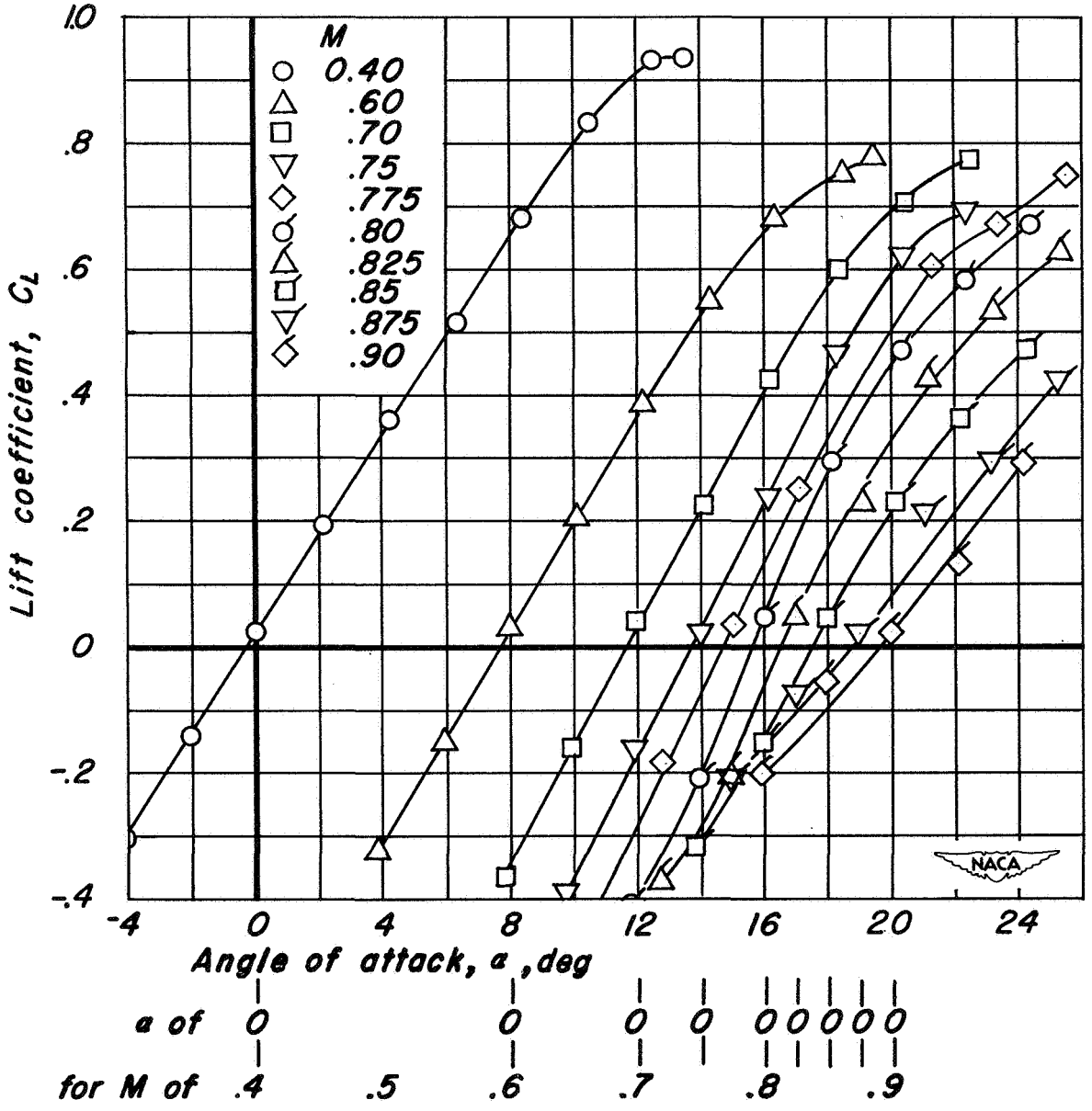

(a) Wing unswept.

Figure 4.- Variation of lift coefficient with angle of attack. Aileron undeflected.

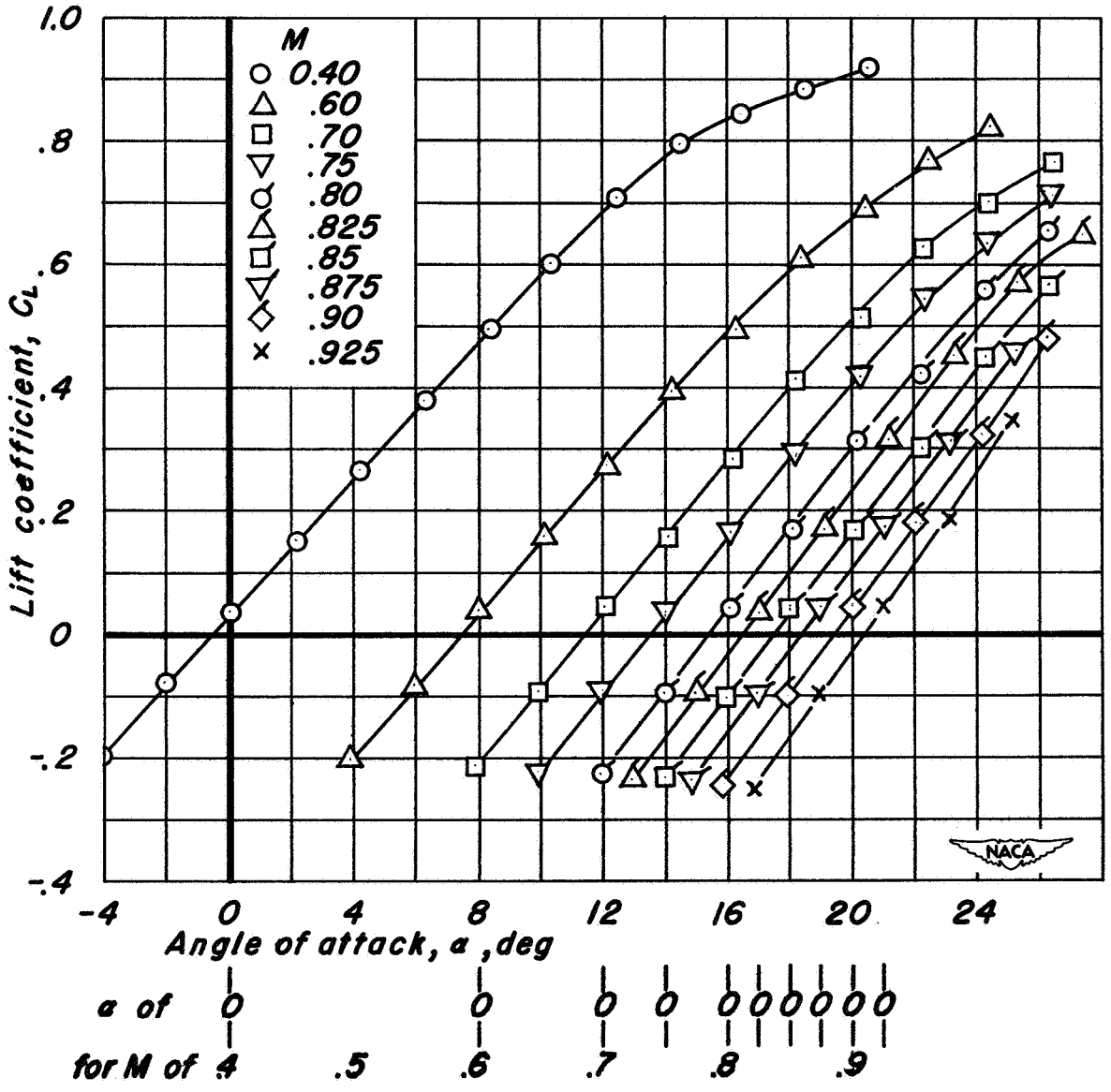

(b) Wing swept back 45°.

Figure 4.- Concluded.

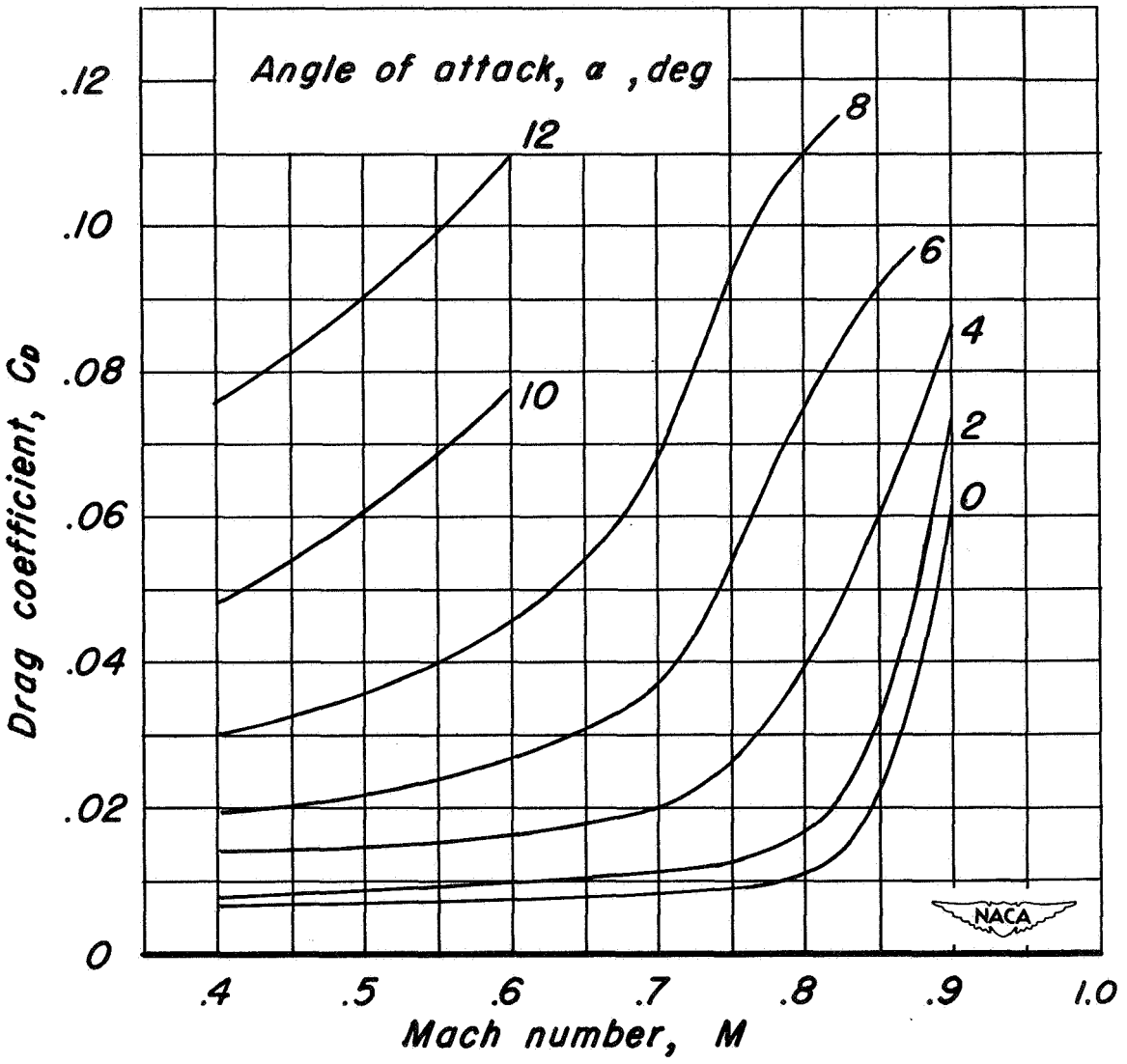

(a) Wing unswept.

Figure 5.- Variation of drag coefficient with Mach number. Aileron undeflected.

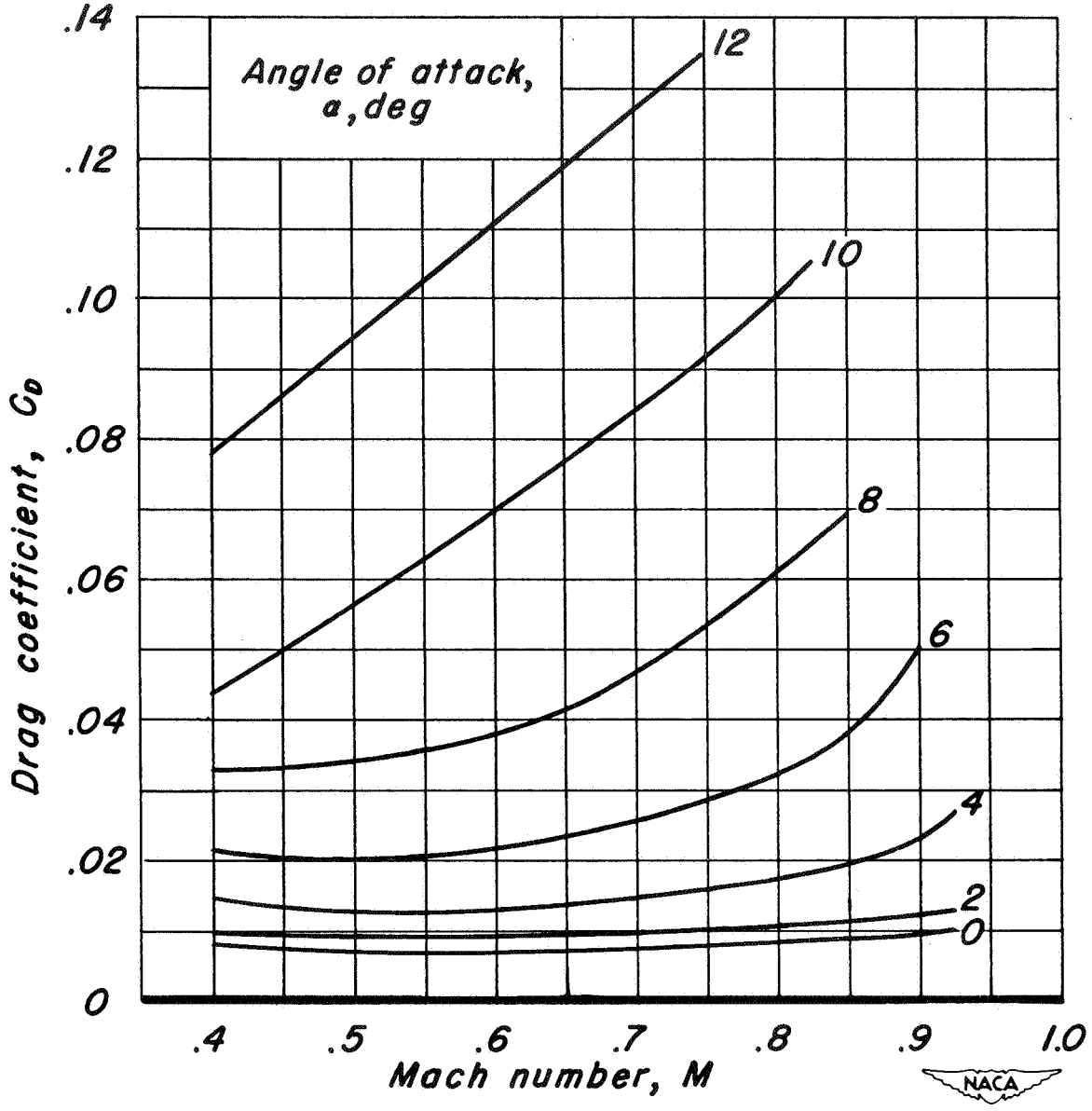

(b) Wing swept back 45°.

Figure 5.- Concluded.

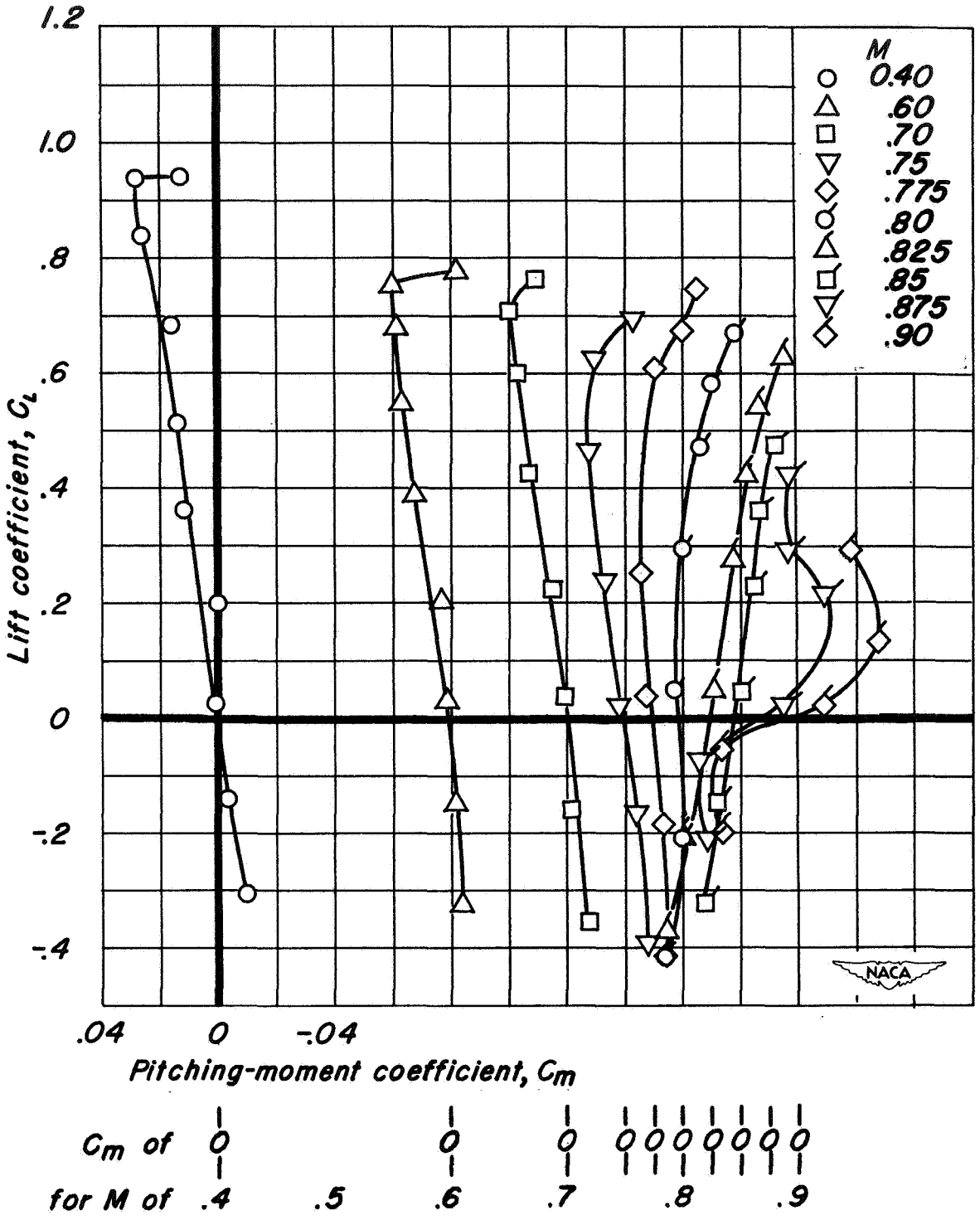

(a) Wing unswept.

Figure 6.- Variation of pitching-moment coefficient with lift coefficient. Aileron undeflected.

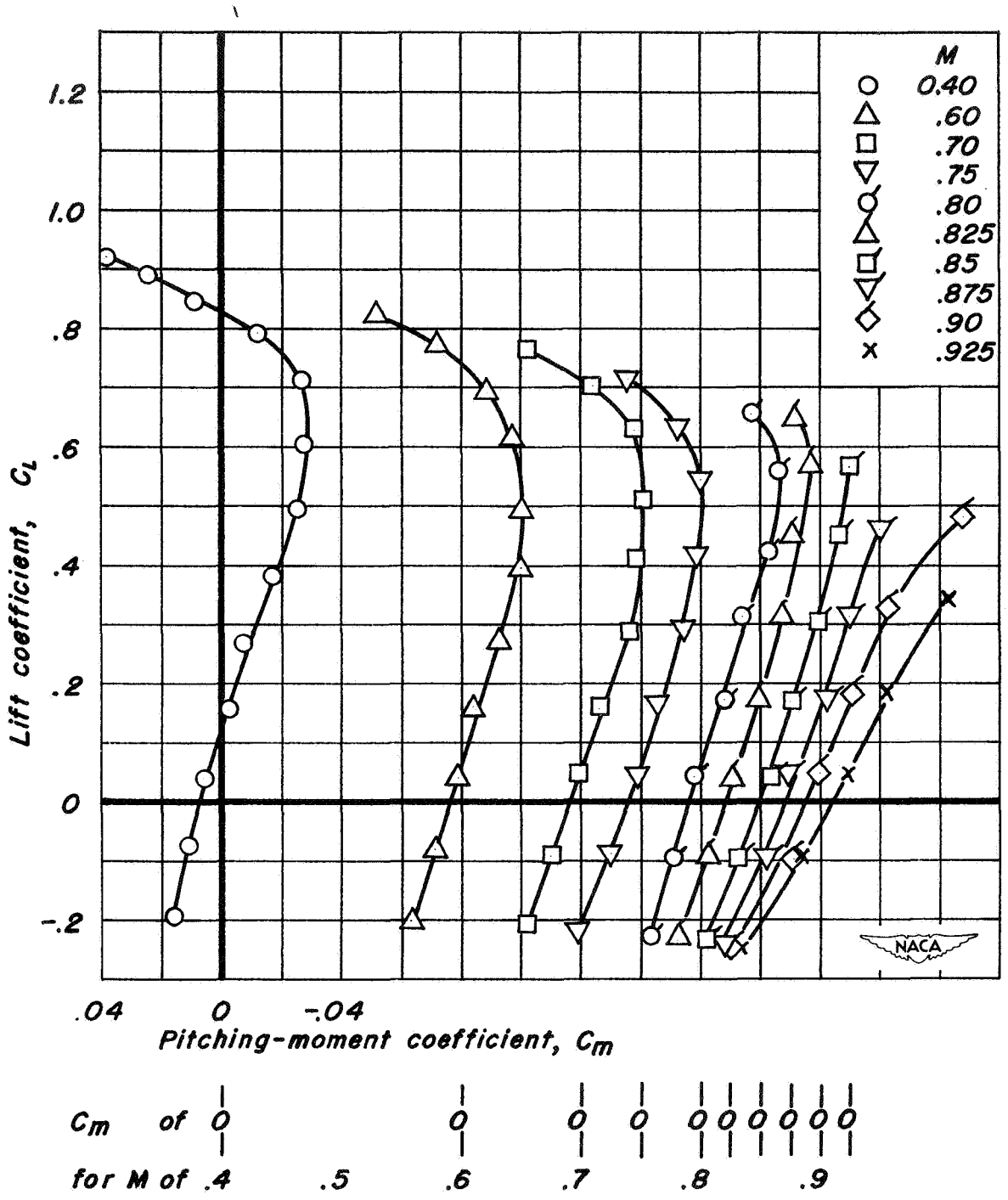

(b) Wing swept back 45°.

Figure 6.- Concluded.

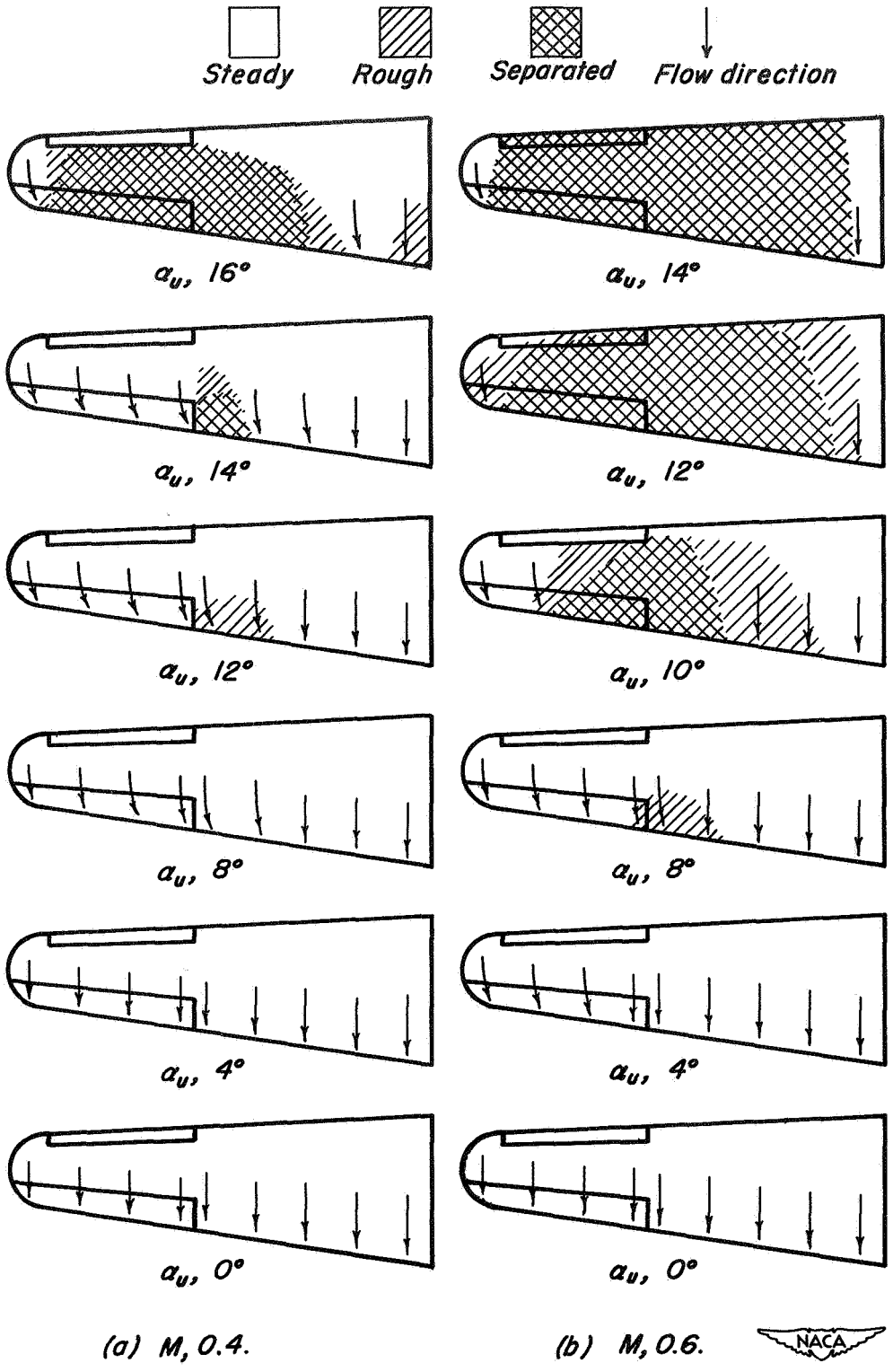

Figure 7.- Stalling characteristics. Wing unswept, aileron undeflected.

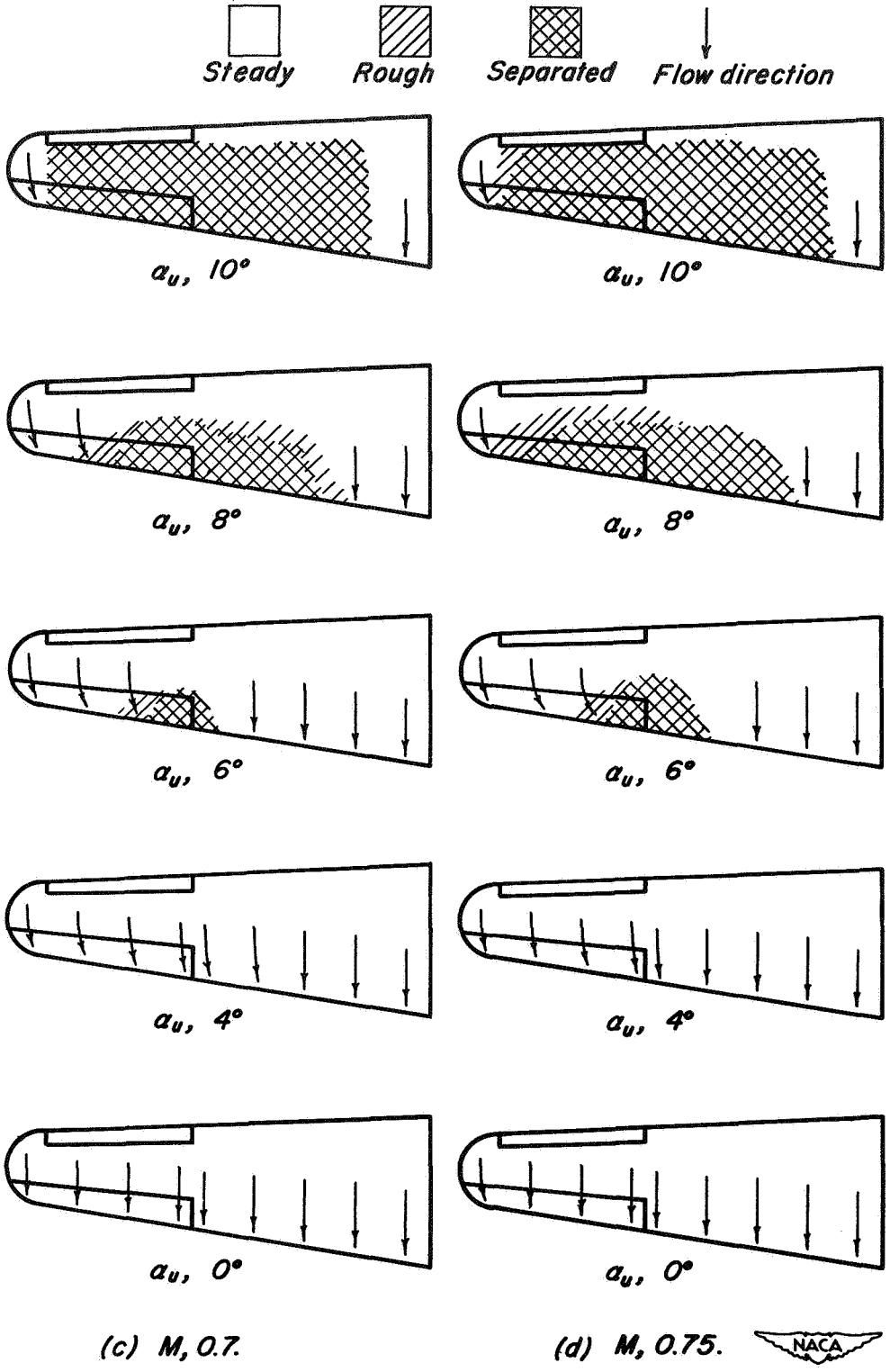

Figure 7.- Continued.

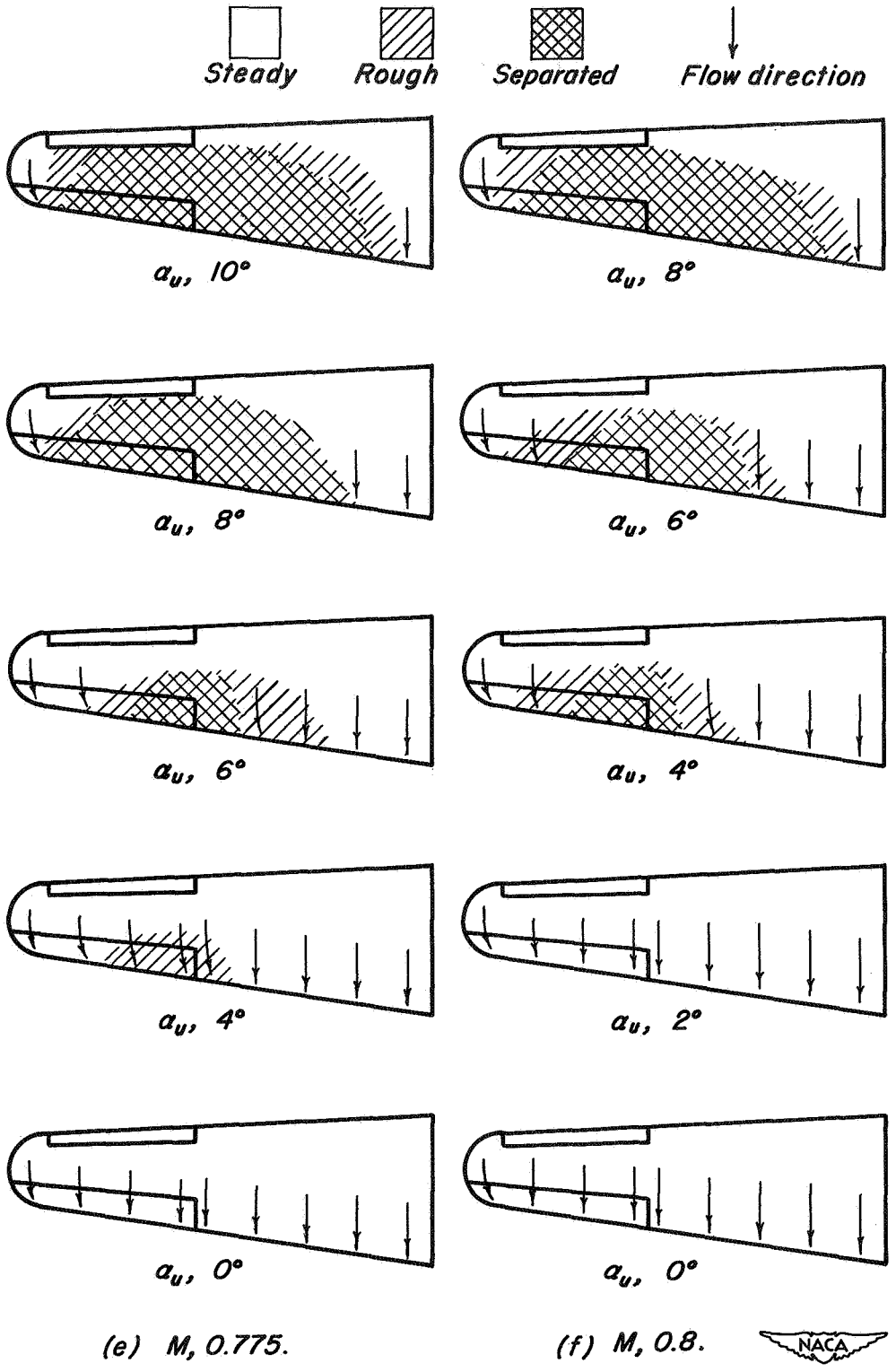

Figure 7.- Continued.

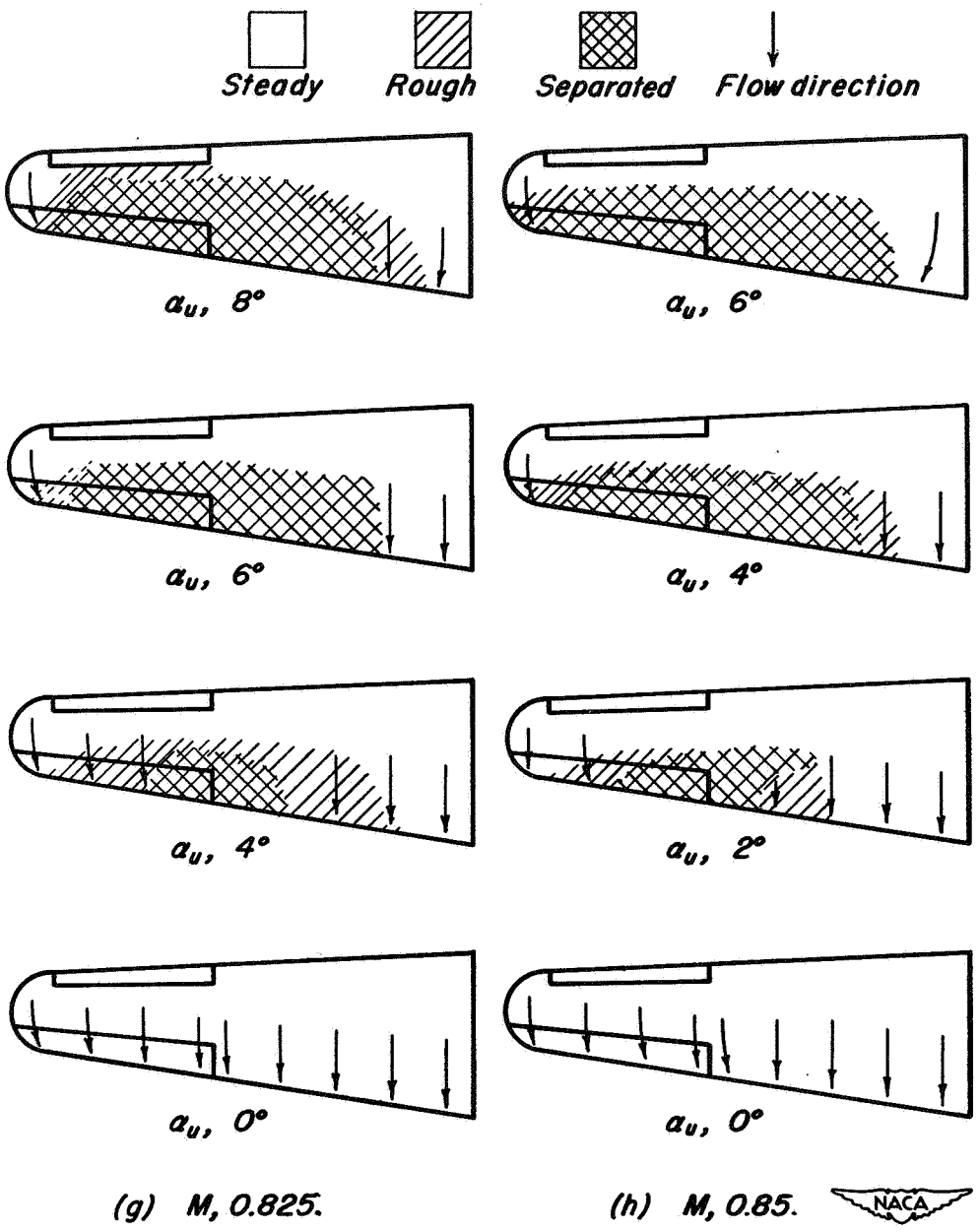

Figure 7.- Continued.

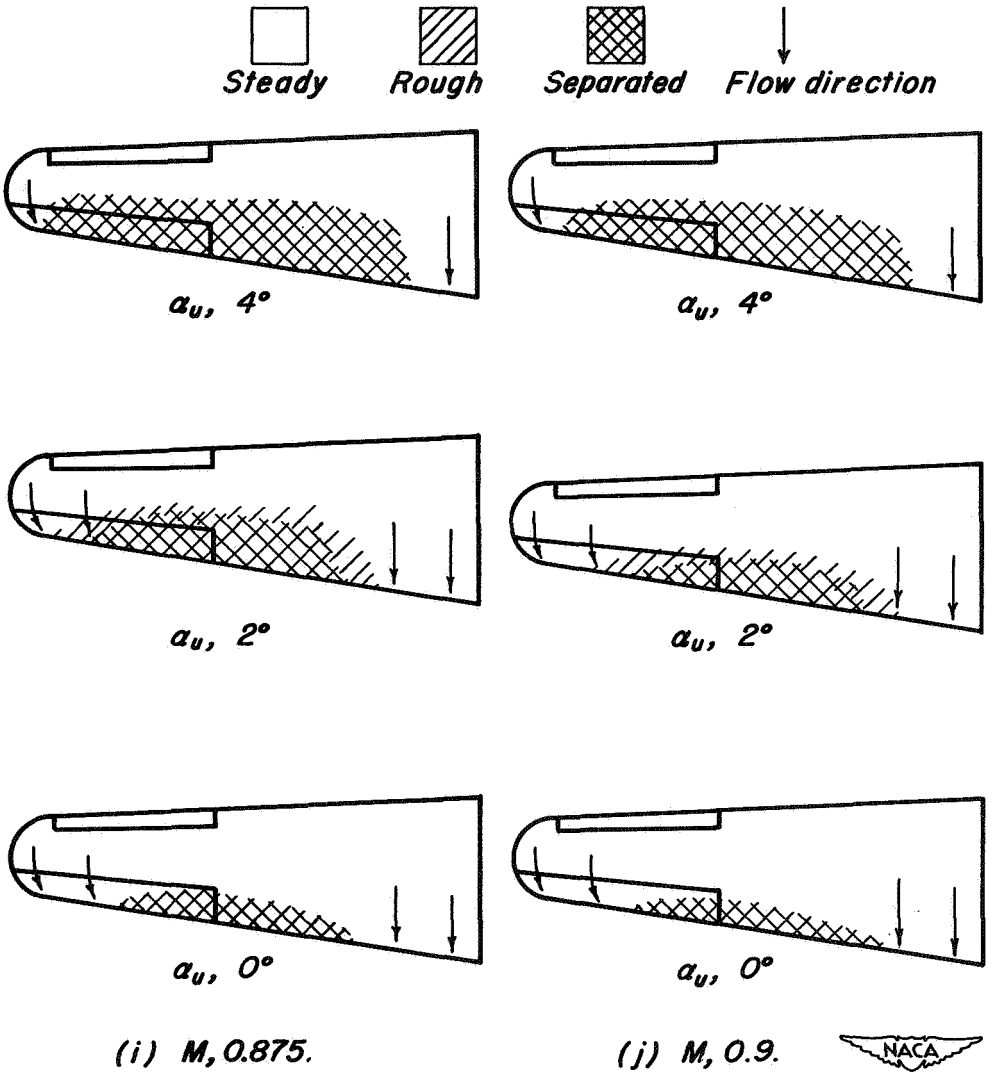

Figure 7.- Concluded.

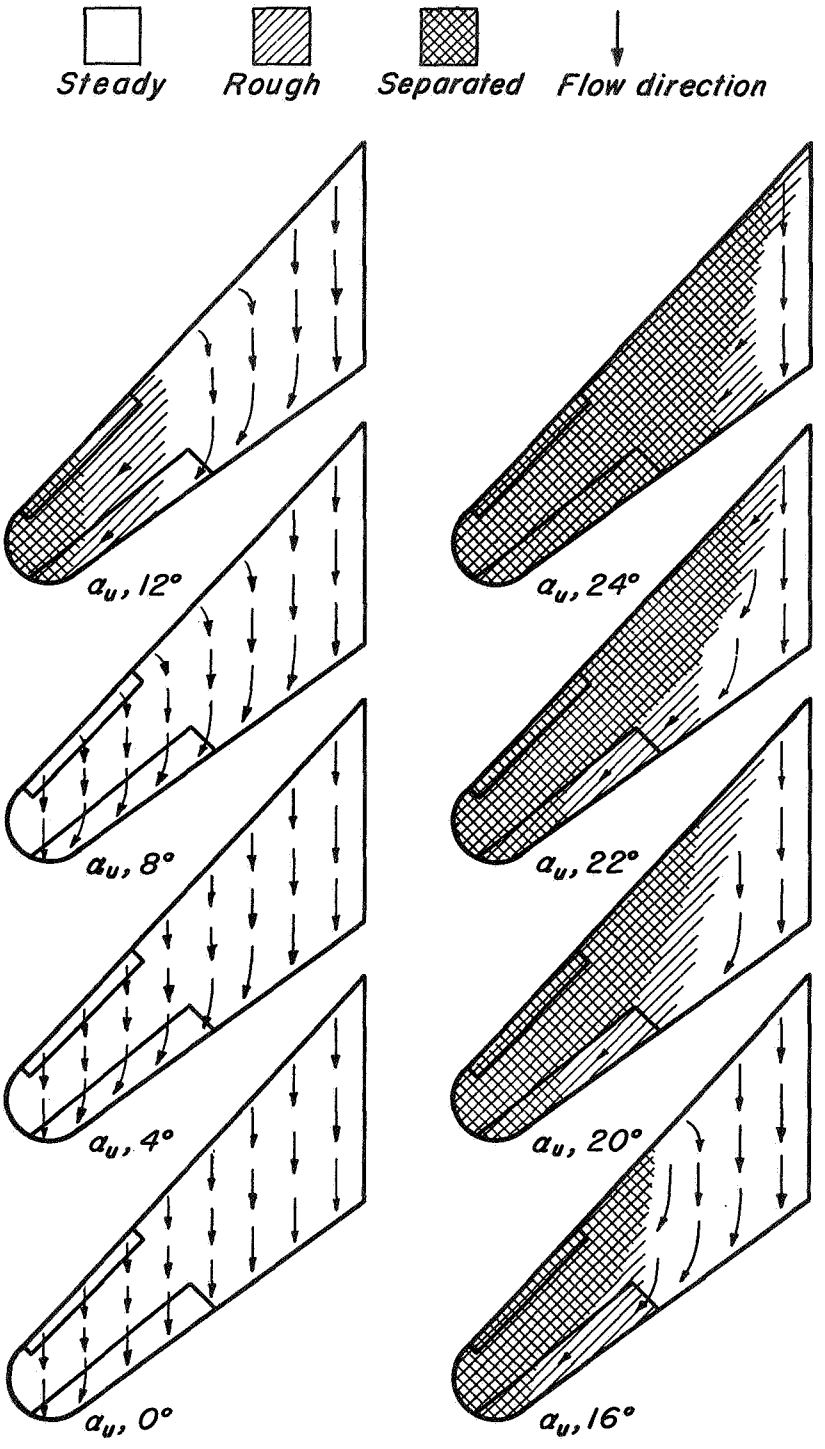

(a) M, 0.4.

Figure 8.- Stalling characteristics. Wing swept back 45°, aileron undeflected.

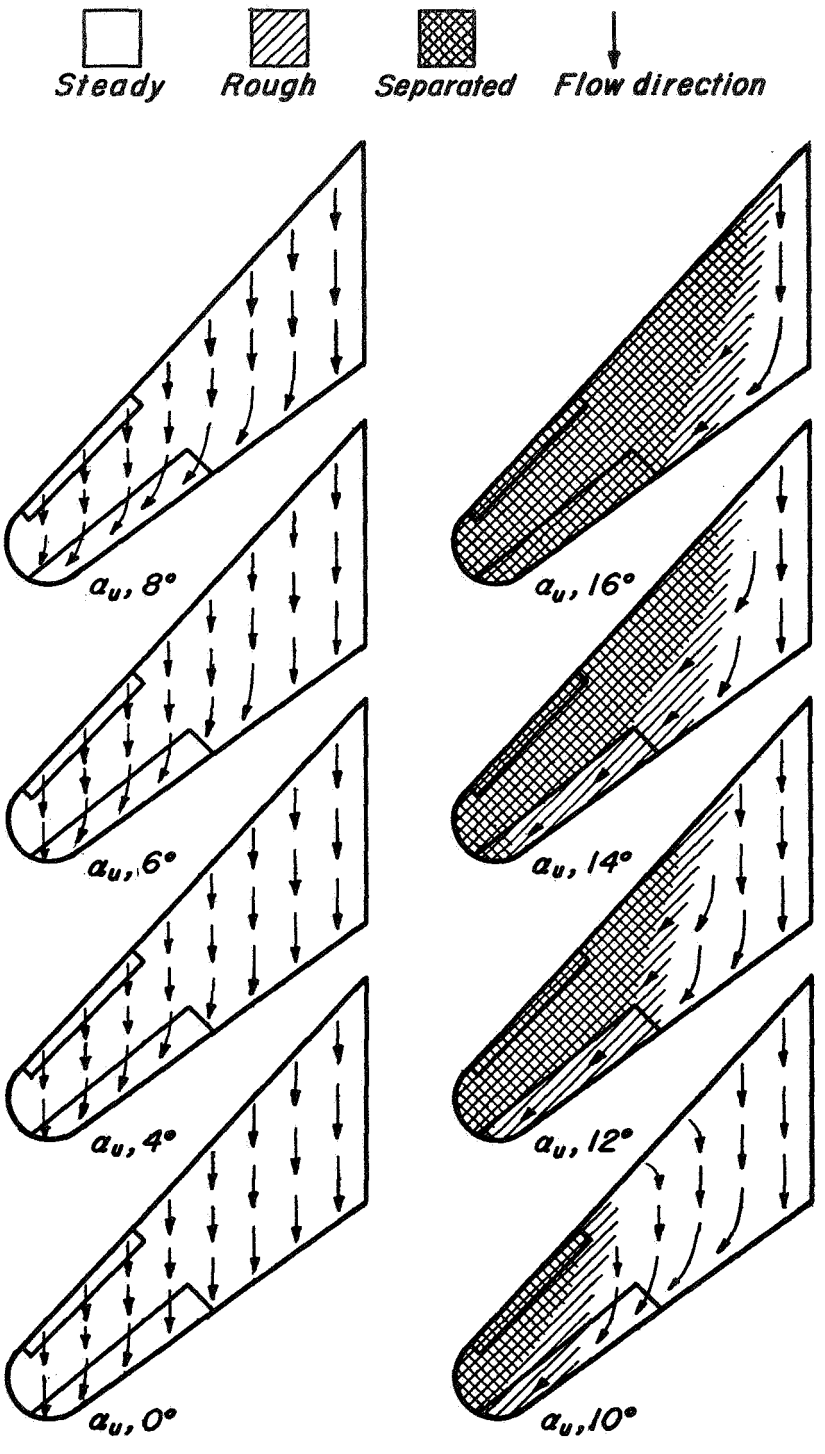

(b) M, 0.6.

Figure 8.- Continued.

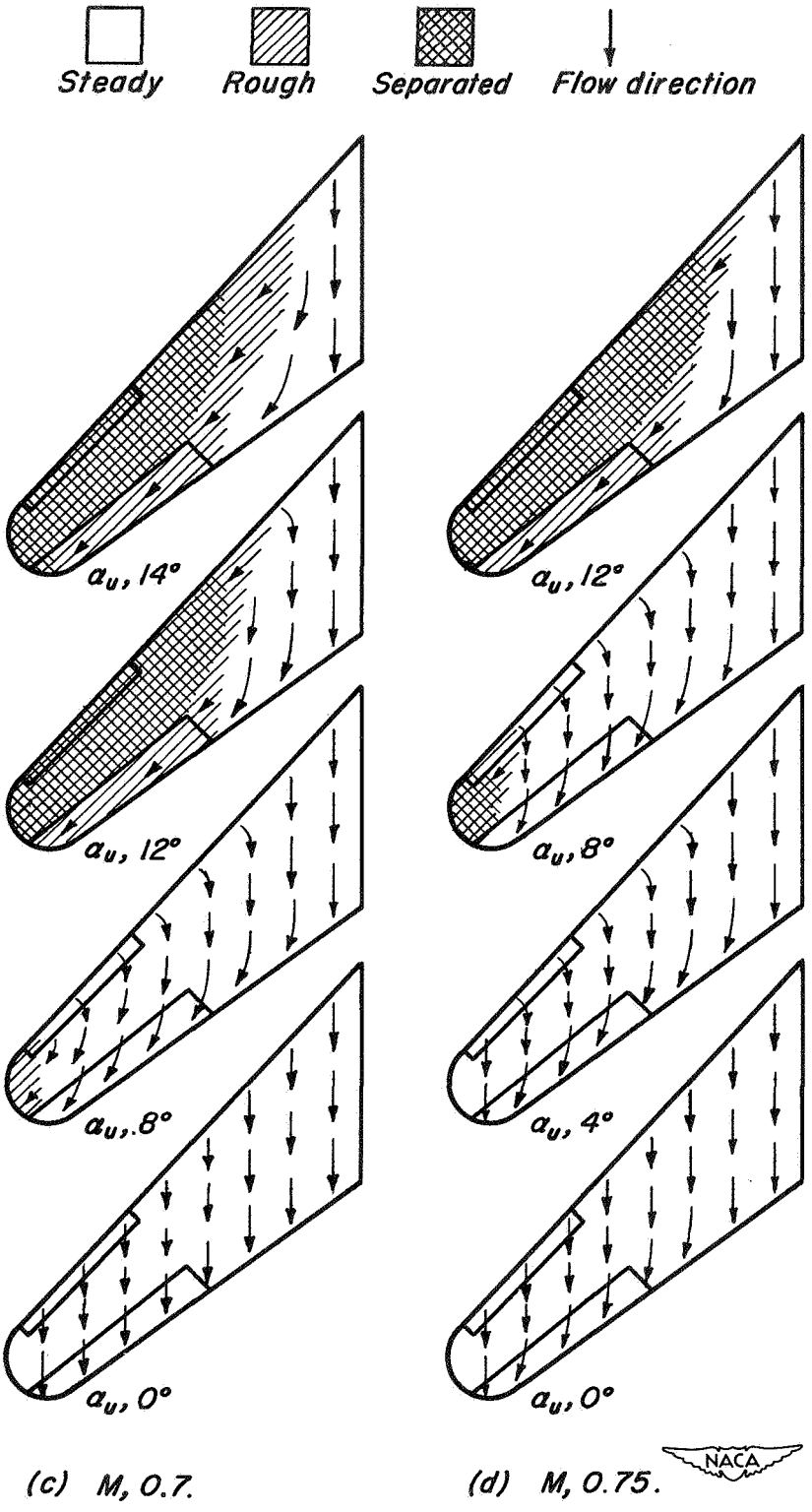

Figure 8.- Continued.

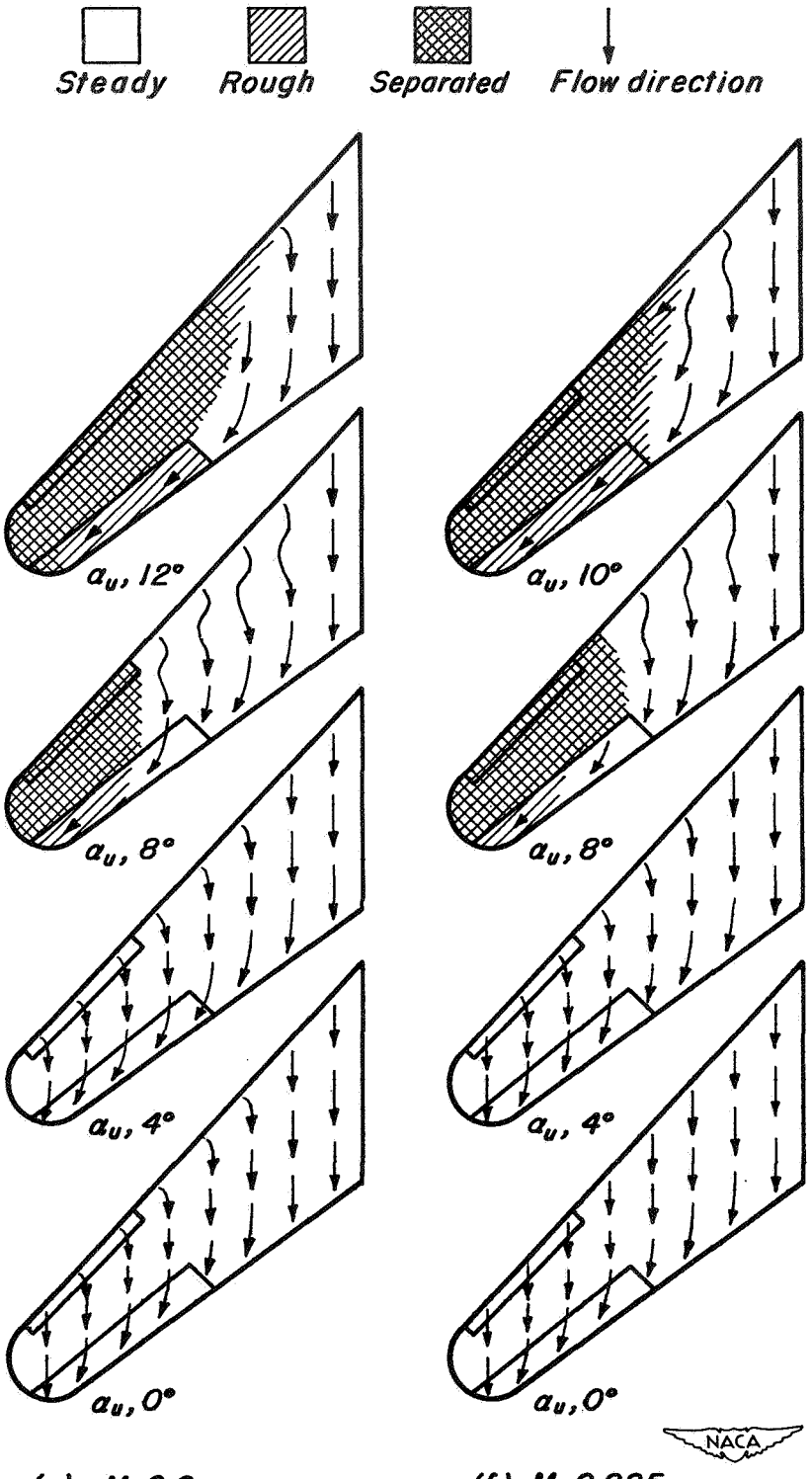

(e) M, 0.8. (f) M, 0.825.

Figure 8.- Continued.

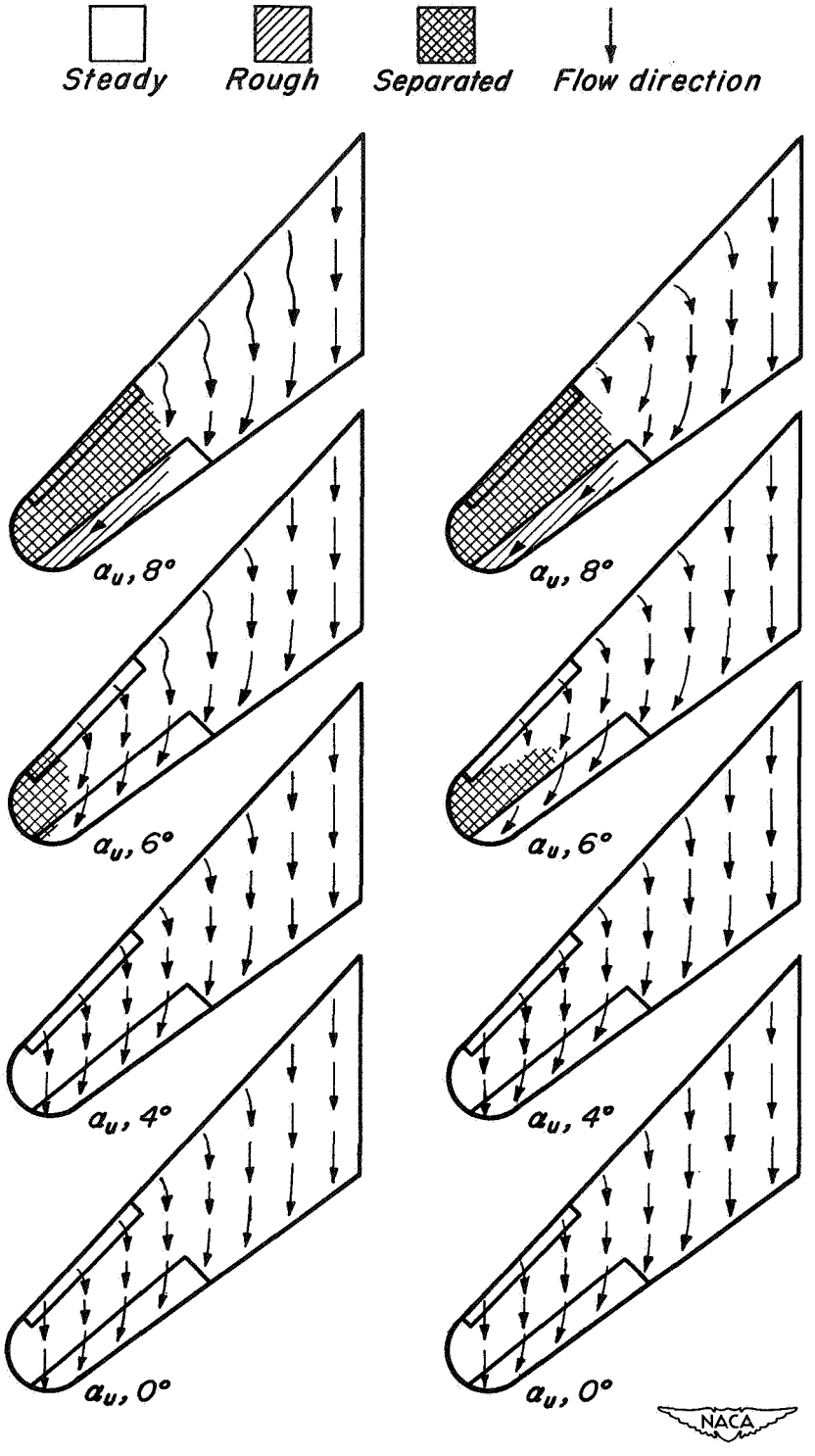

(g) M, 0.85. (h) M, 0.875.

Figure 8.- Continued.

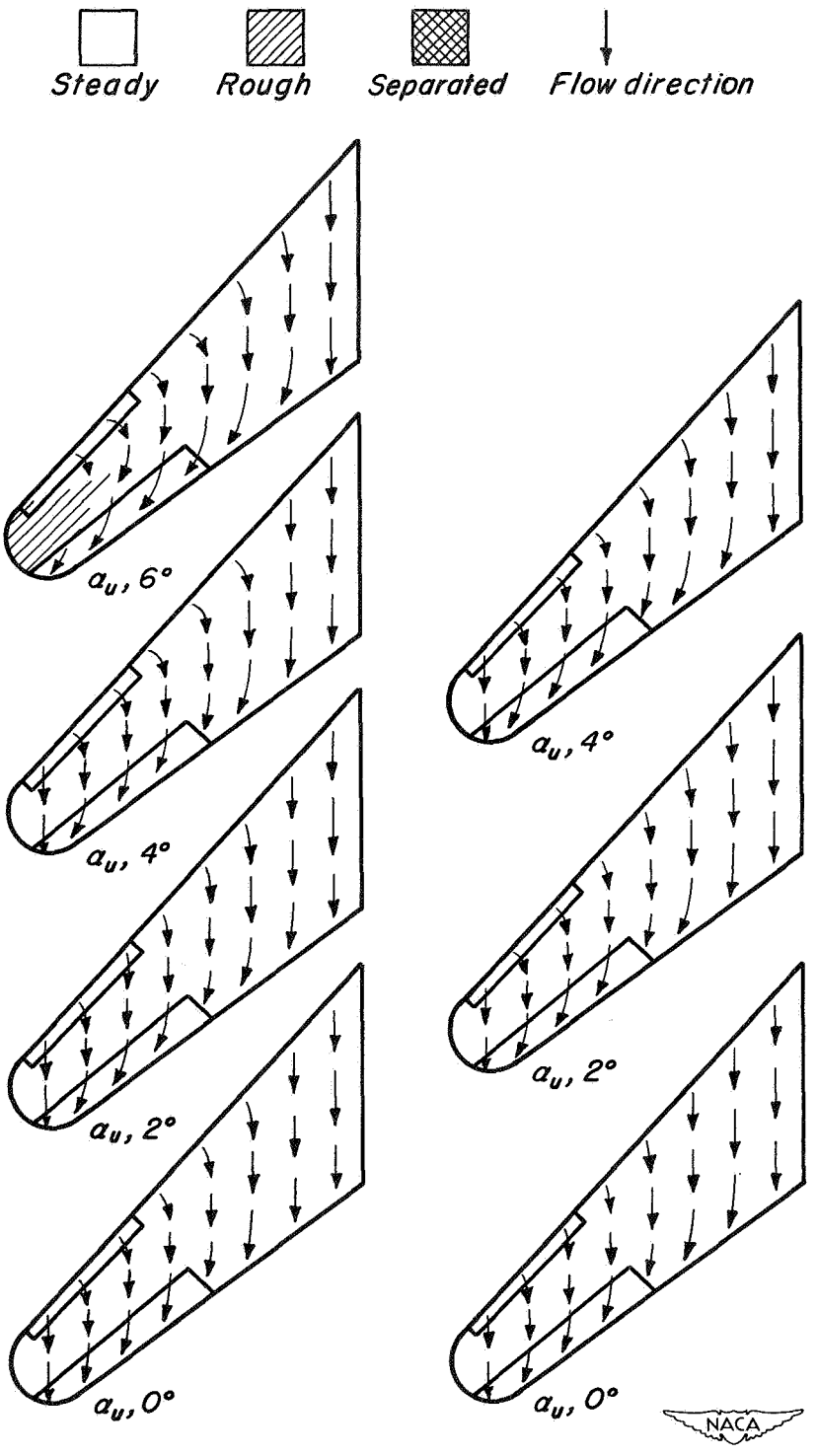

(i) M, 0.9. (j) M, 0.925.

Figure 8.- Concluded.

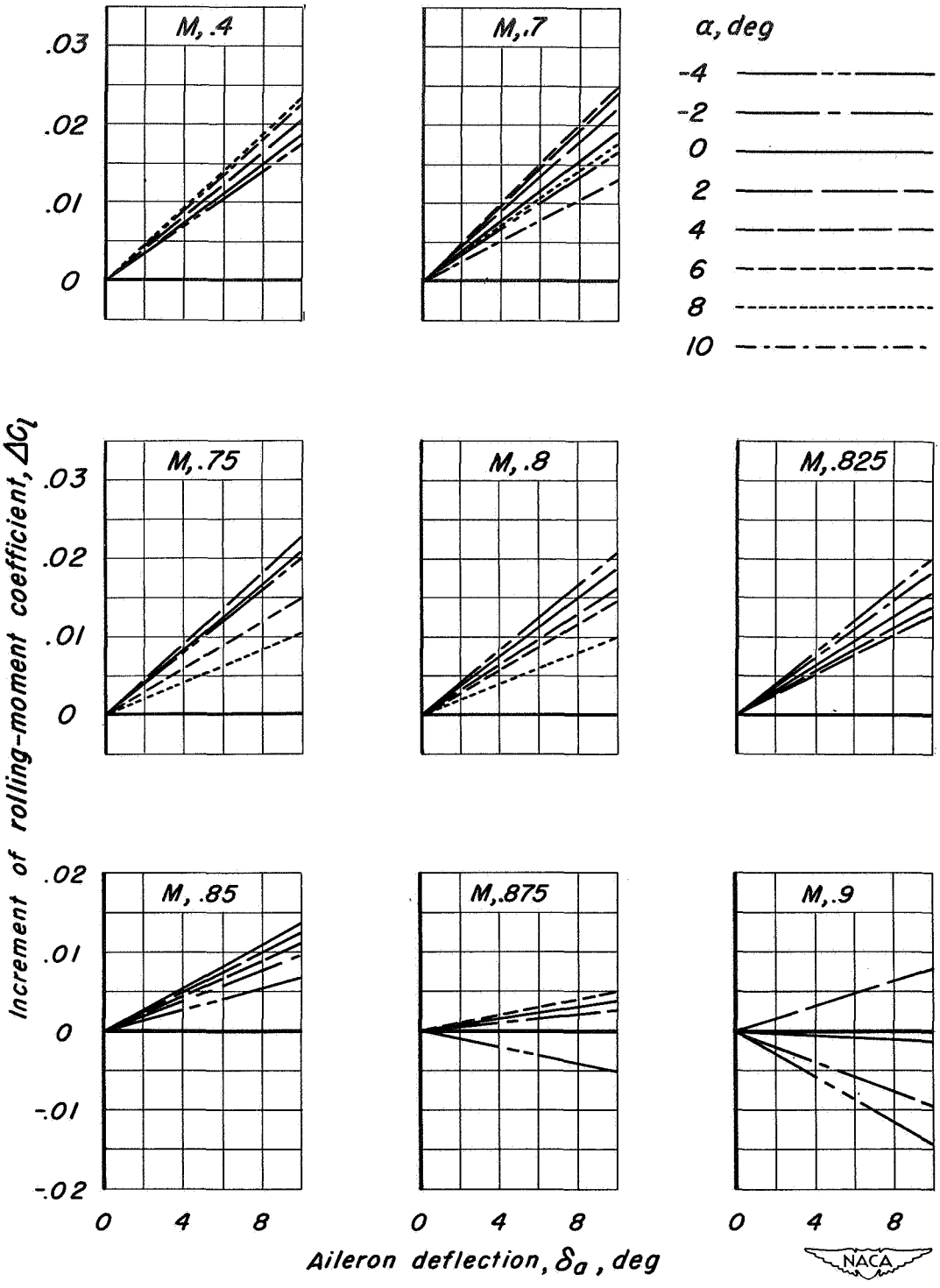

(a) Wing unswept.

Figure 9.- Variation of increment of rolling-moment coefficient with trailing-edge aileron deflection.

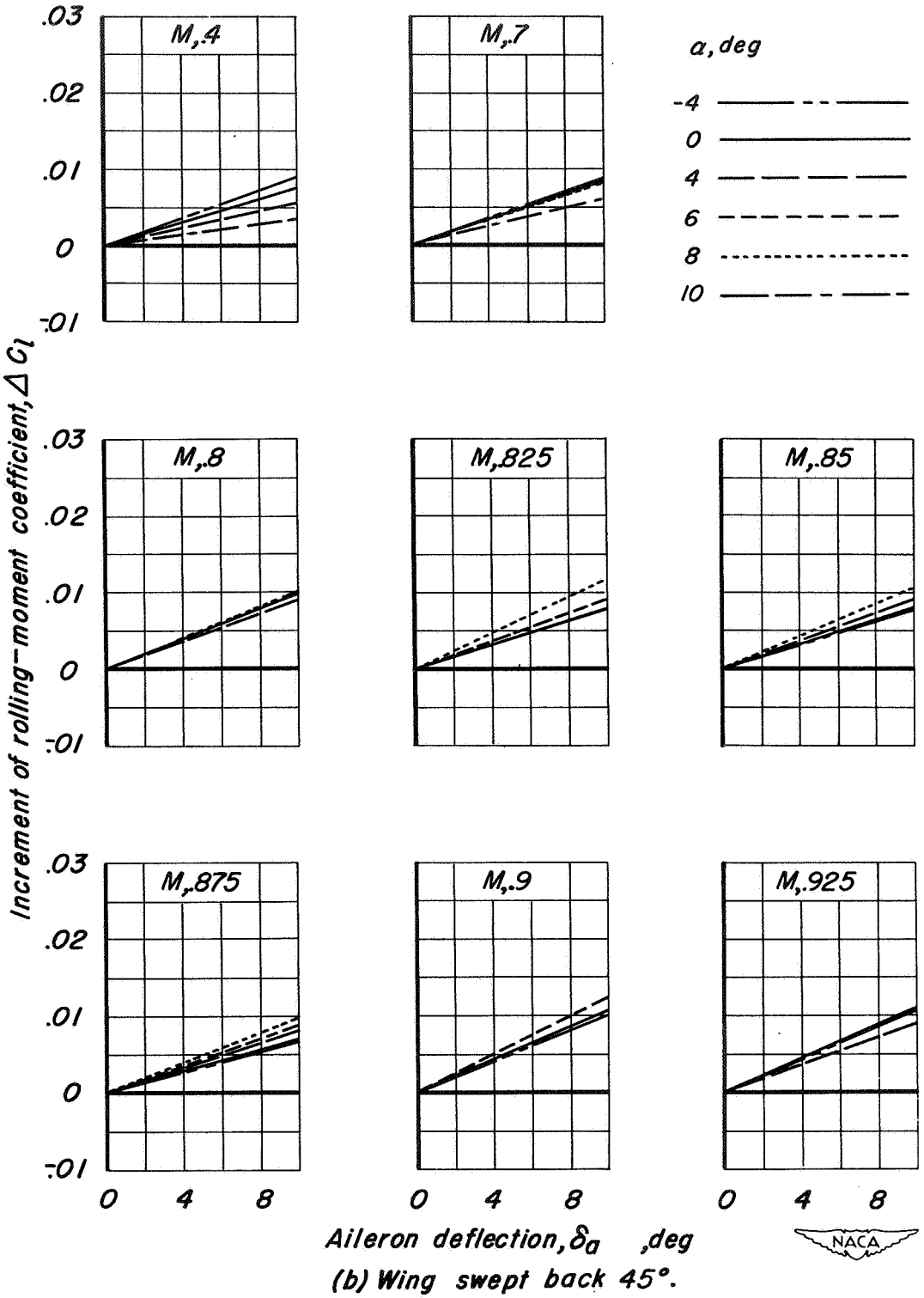

(b) Wing swept back 45°.

Figure 9.– Concluded.

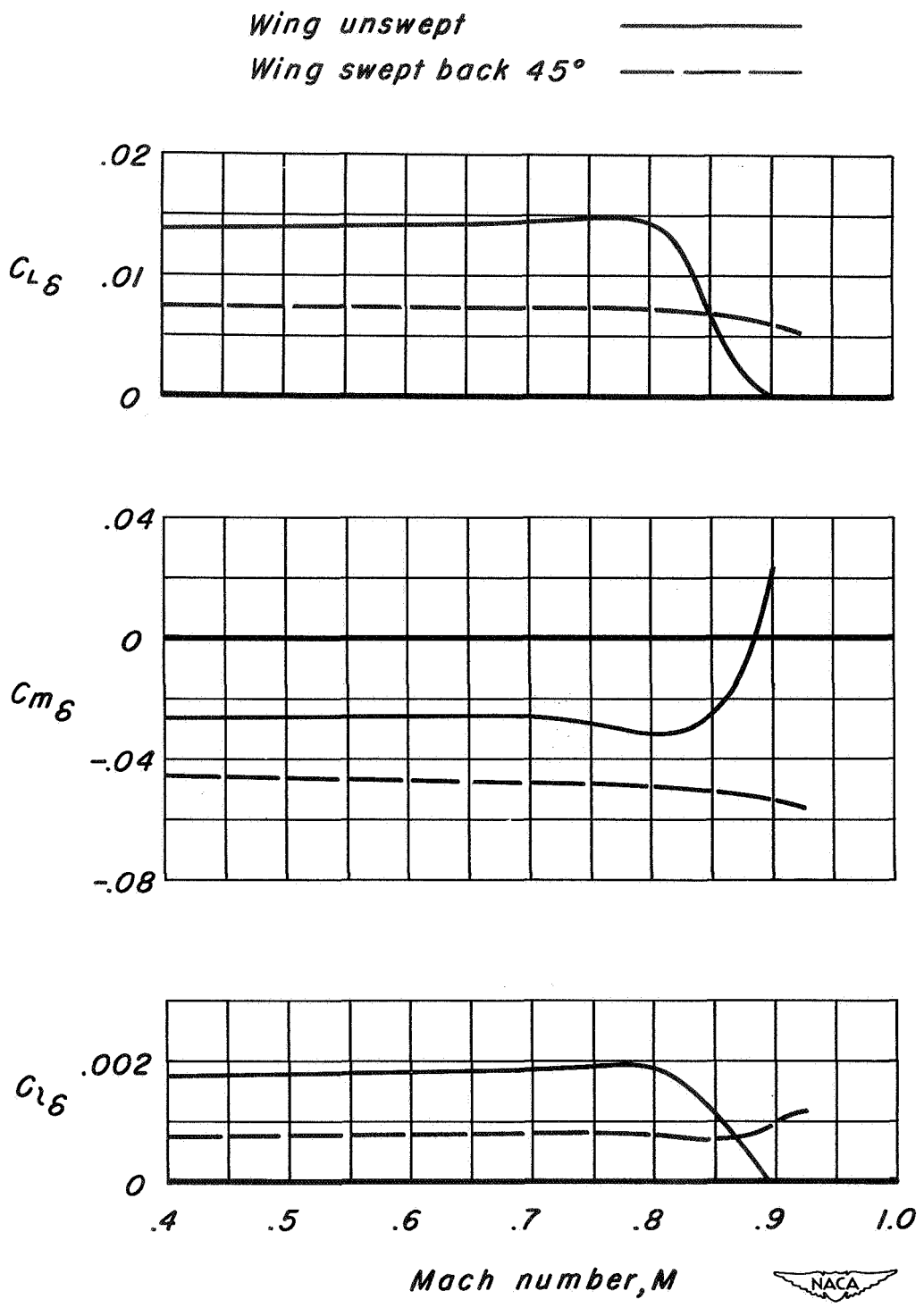

Figure 10.– Variation of the trailing-edge aileron effectiveness parameters with Mach number.

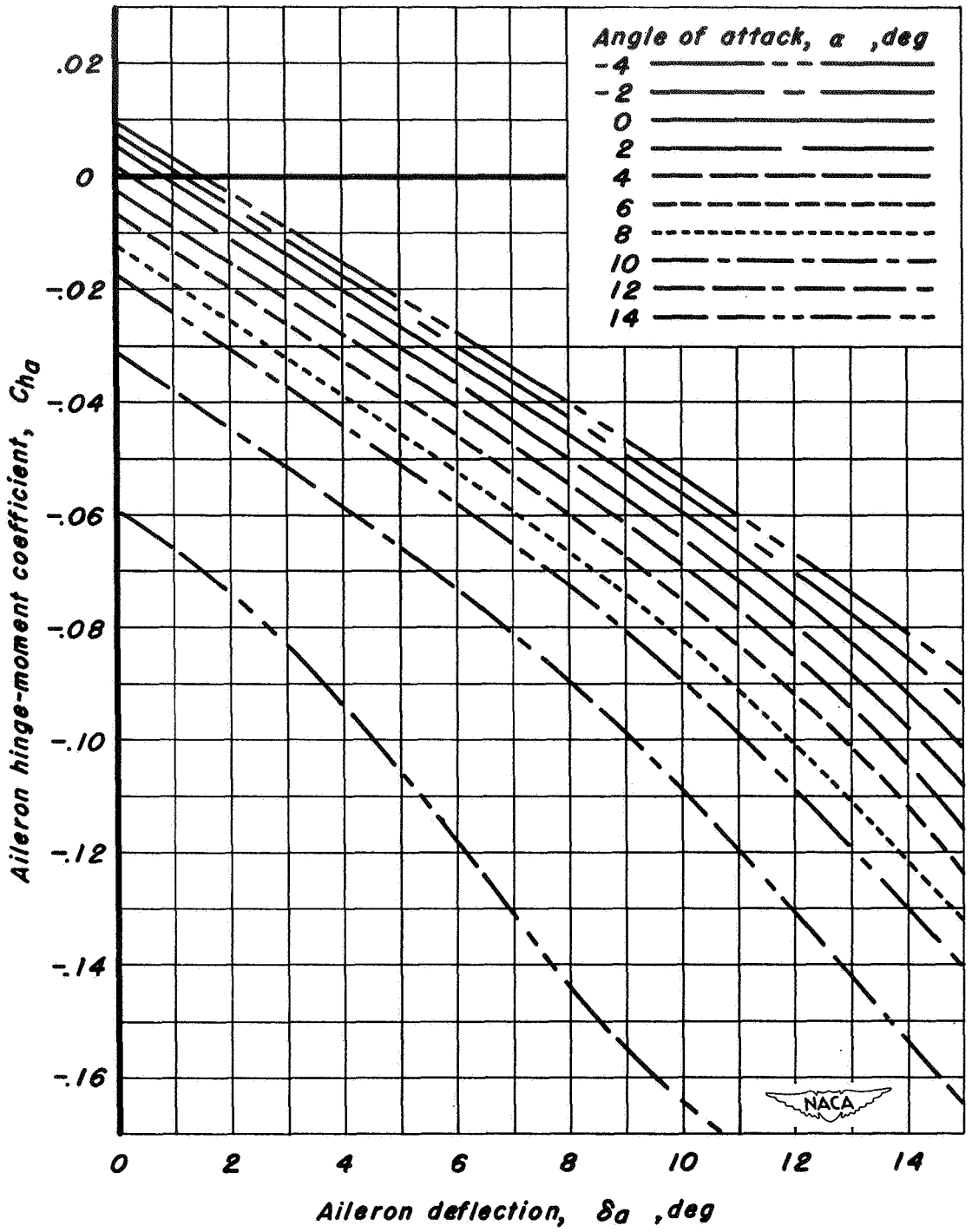

(a) M, 0.40.

Figure 11.- Variation of trailing-edge aileron hinge-moment coefficient with trailing-edge aileron deflection. Wing unswept.

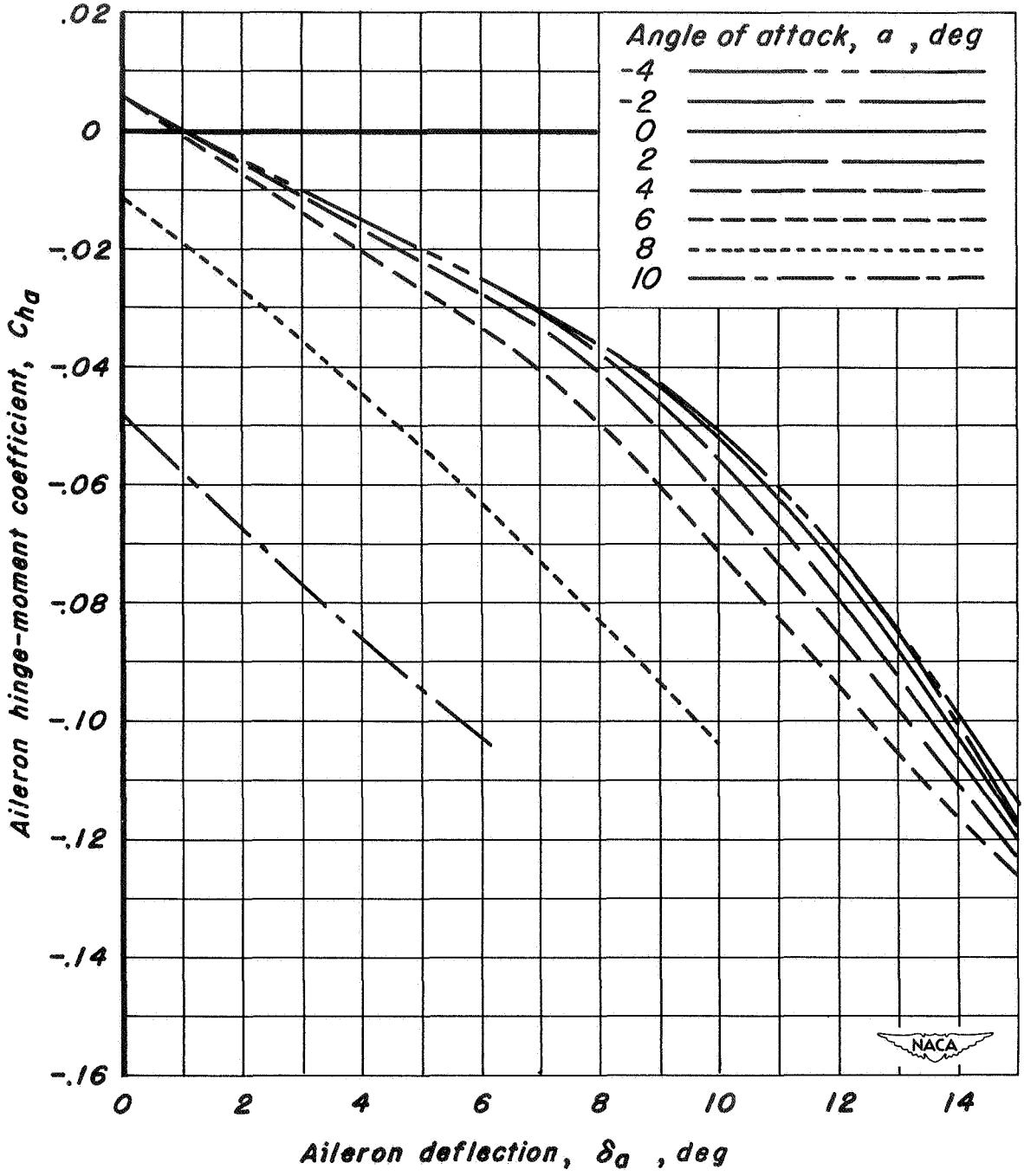

(b) M, 0.70.

Figure 11.– Continued.

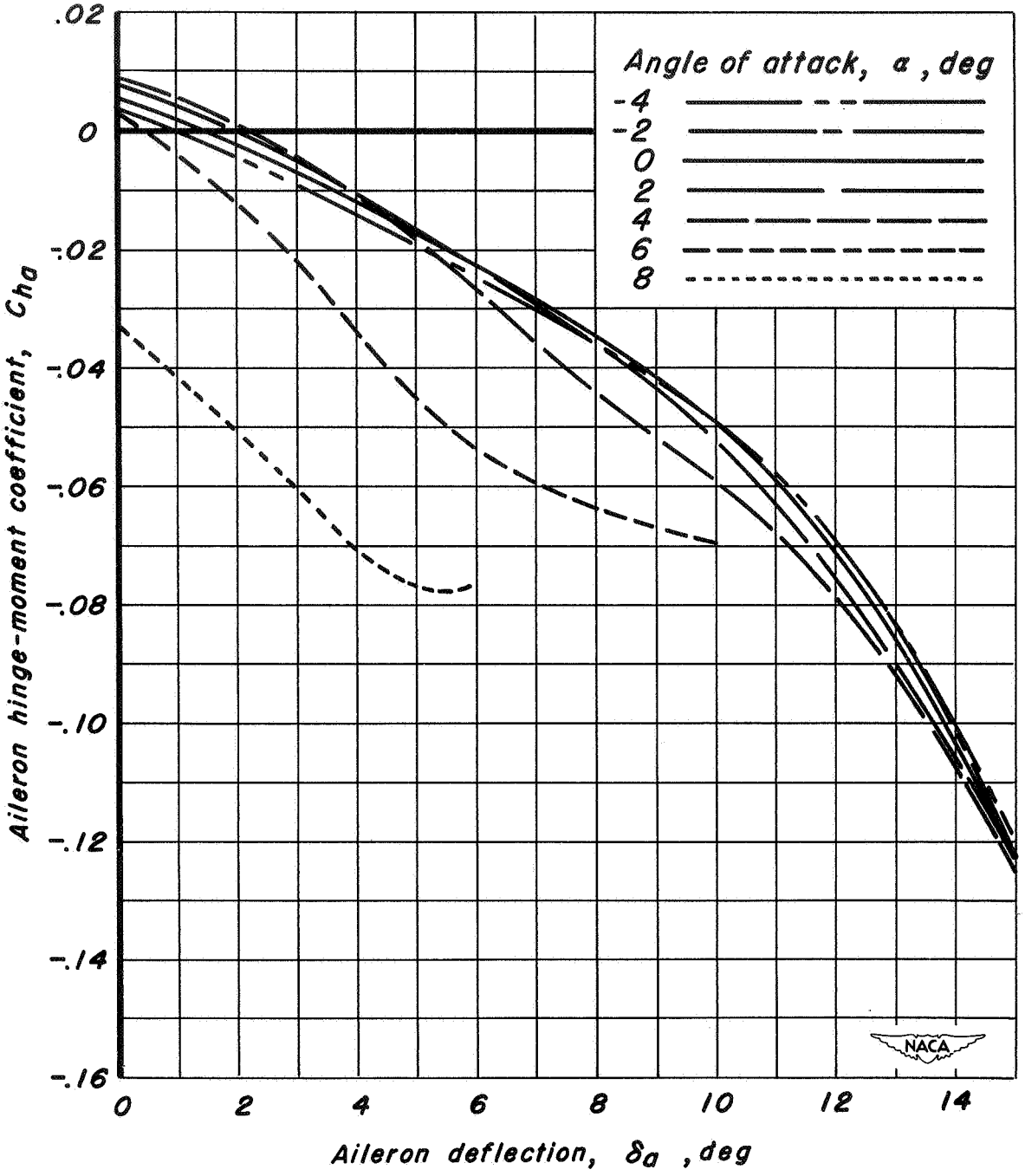

(c) M, 0.75.

Figure 11.- Continued.

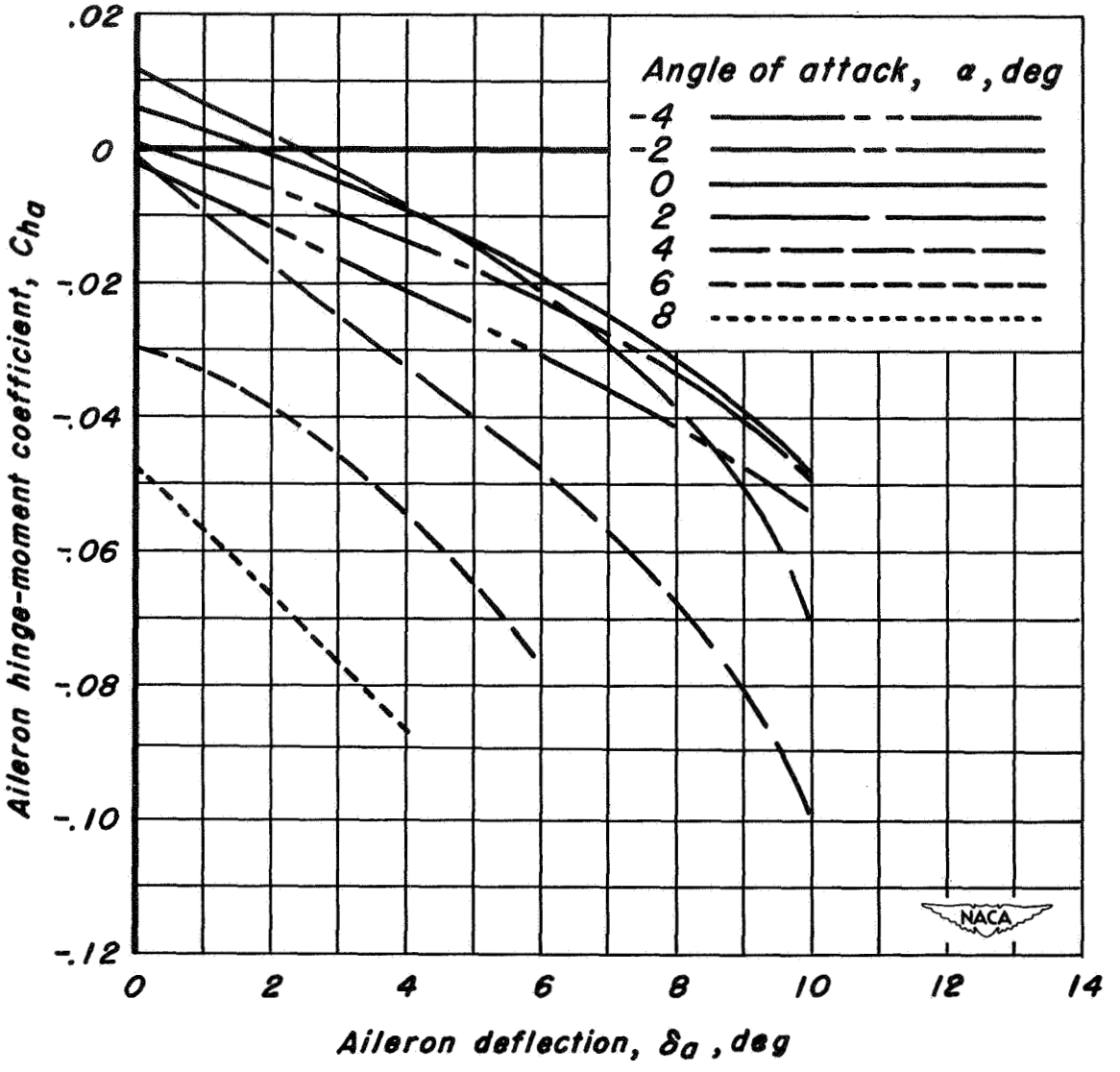

(d) M, 0.80.

Figure 11.- Continued.

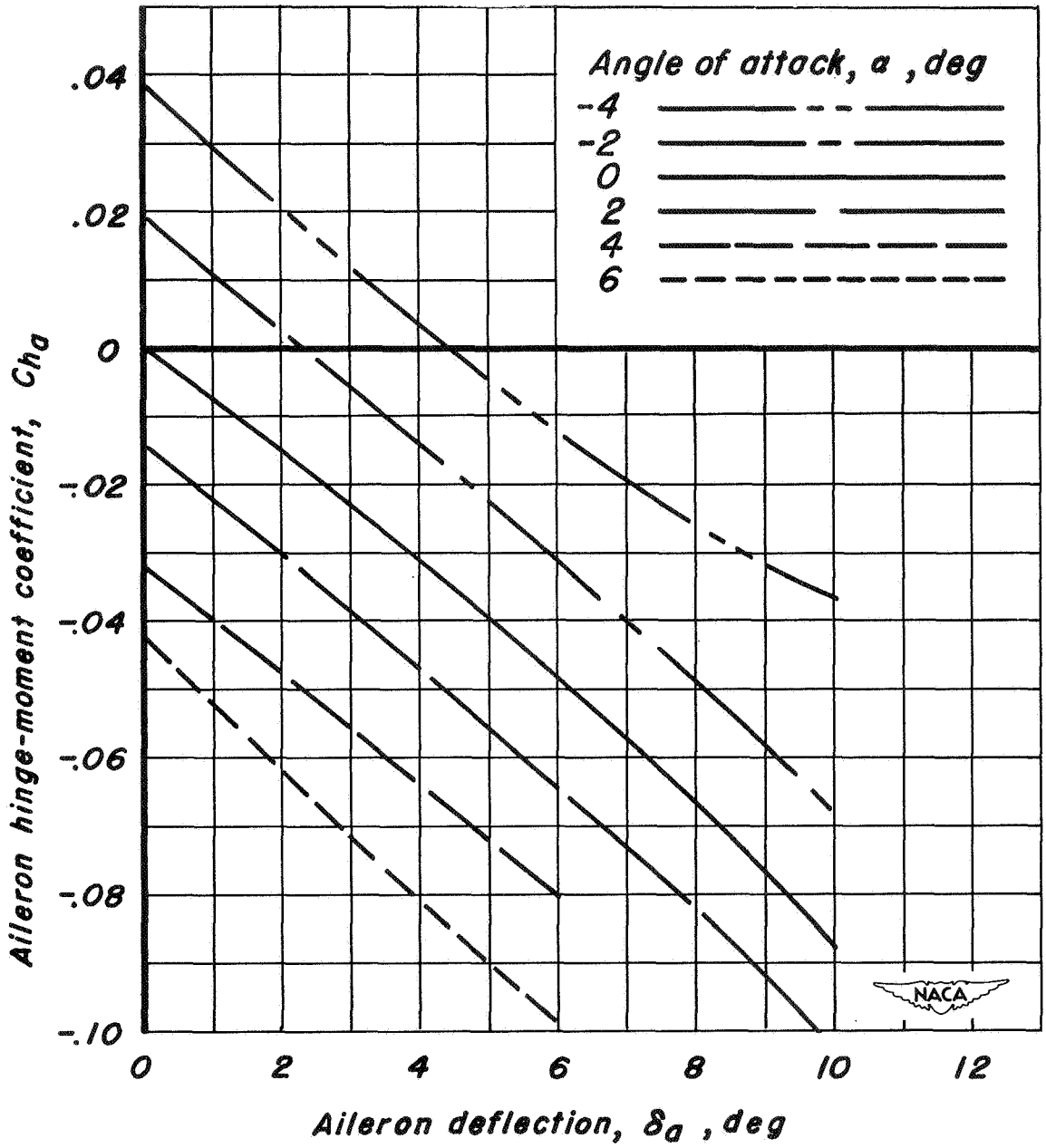

(e) M, 0.825.

Figure 11.- Continued.

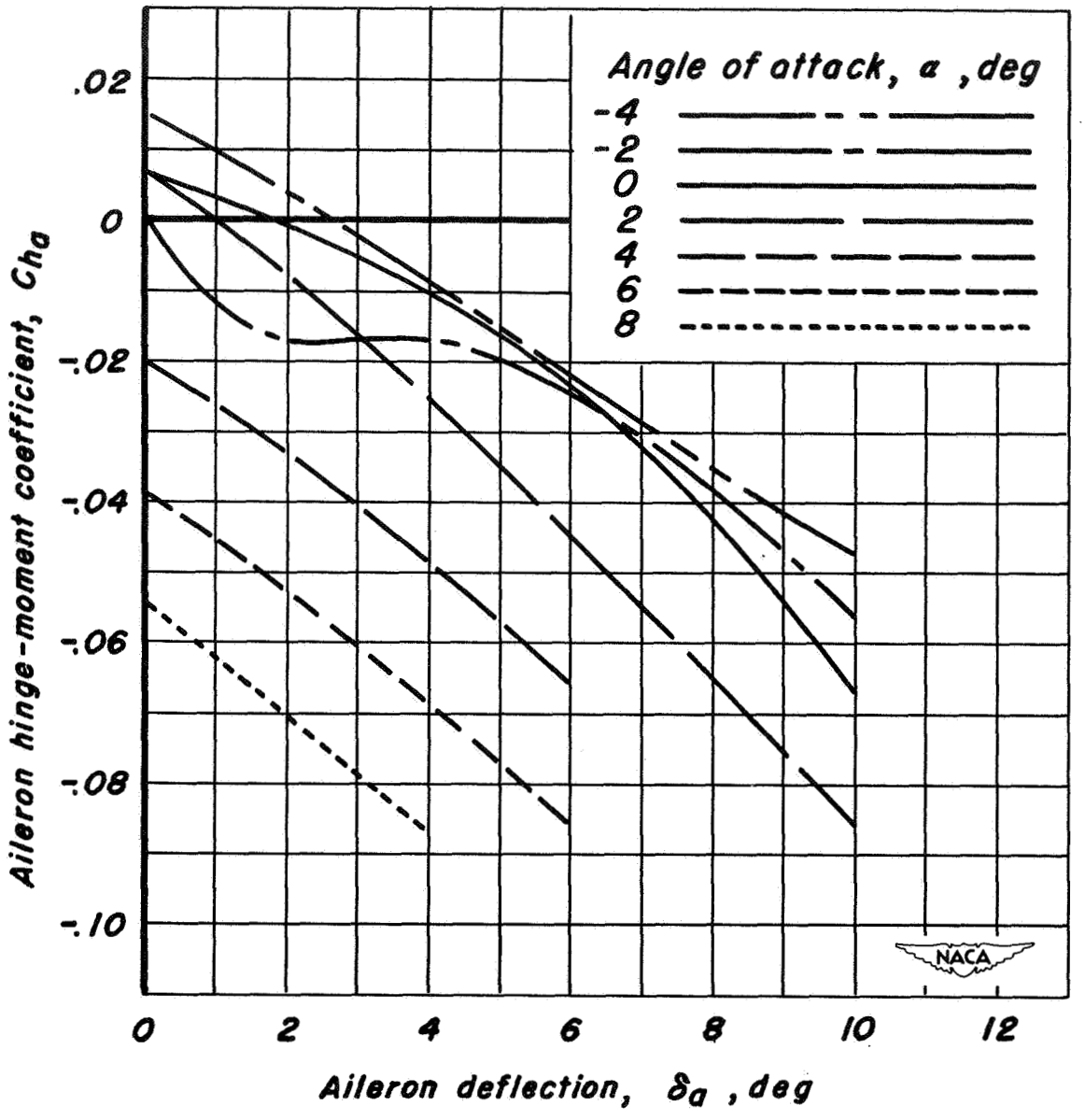

(f) M, 0.85.

Figure 11.- Continued.

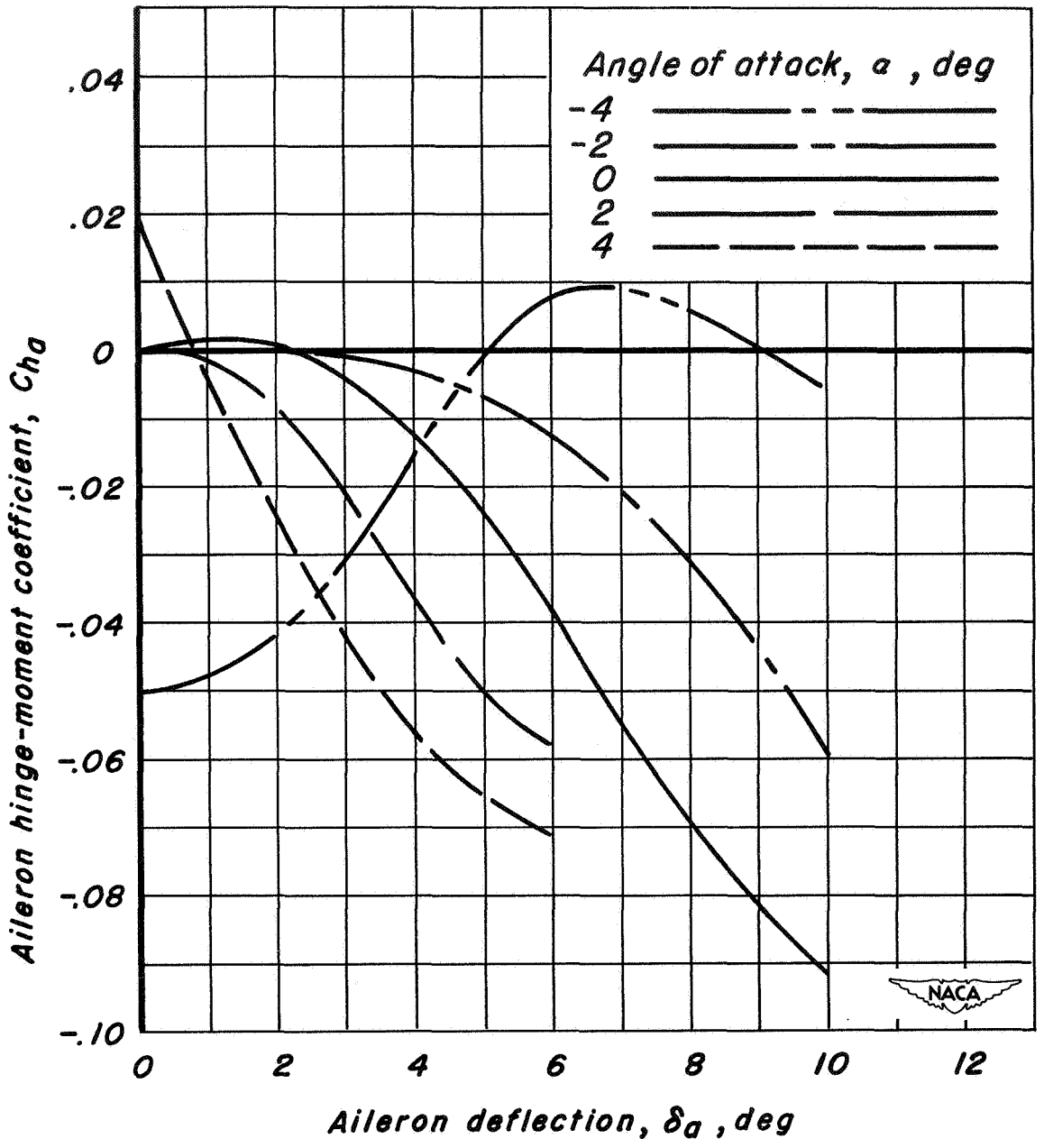

(g) M, 0.875.

Figure 11.- Continued.

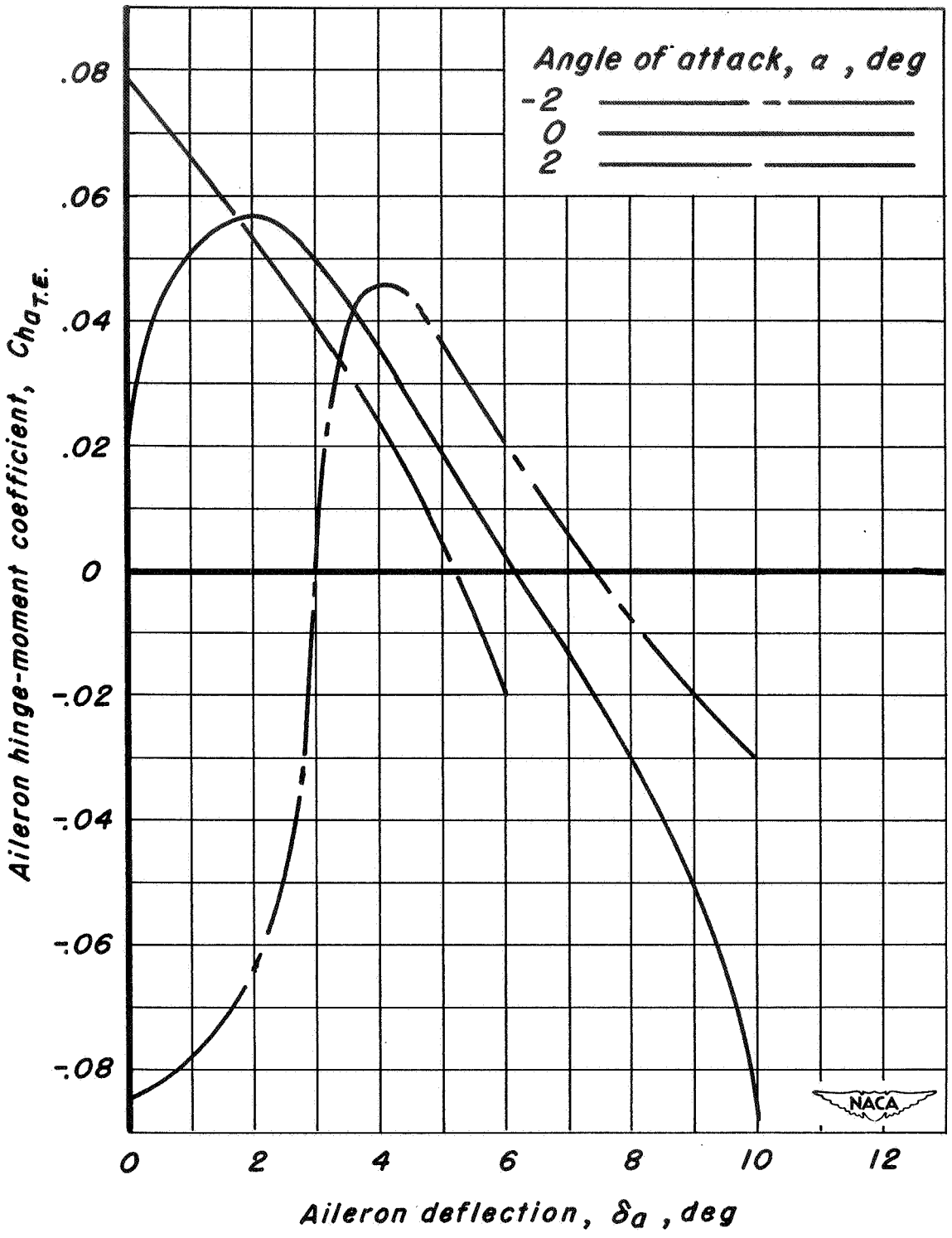

(h) M, 0.90.

Figure 11.- Concluded.

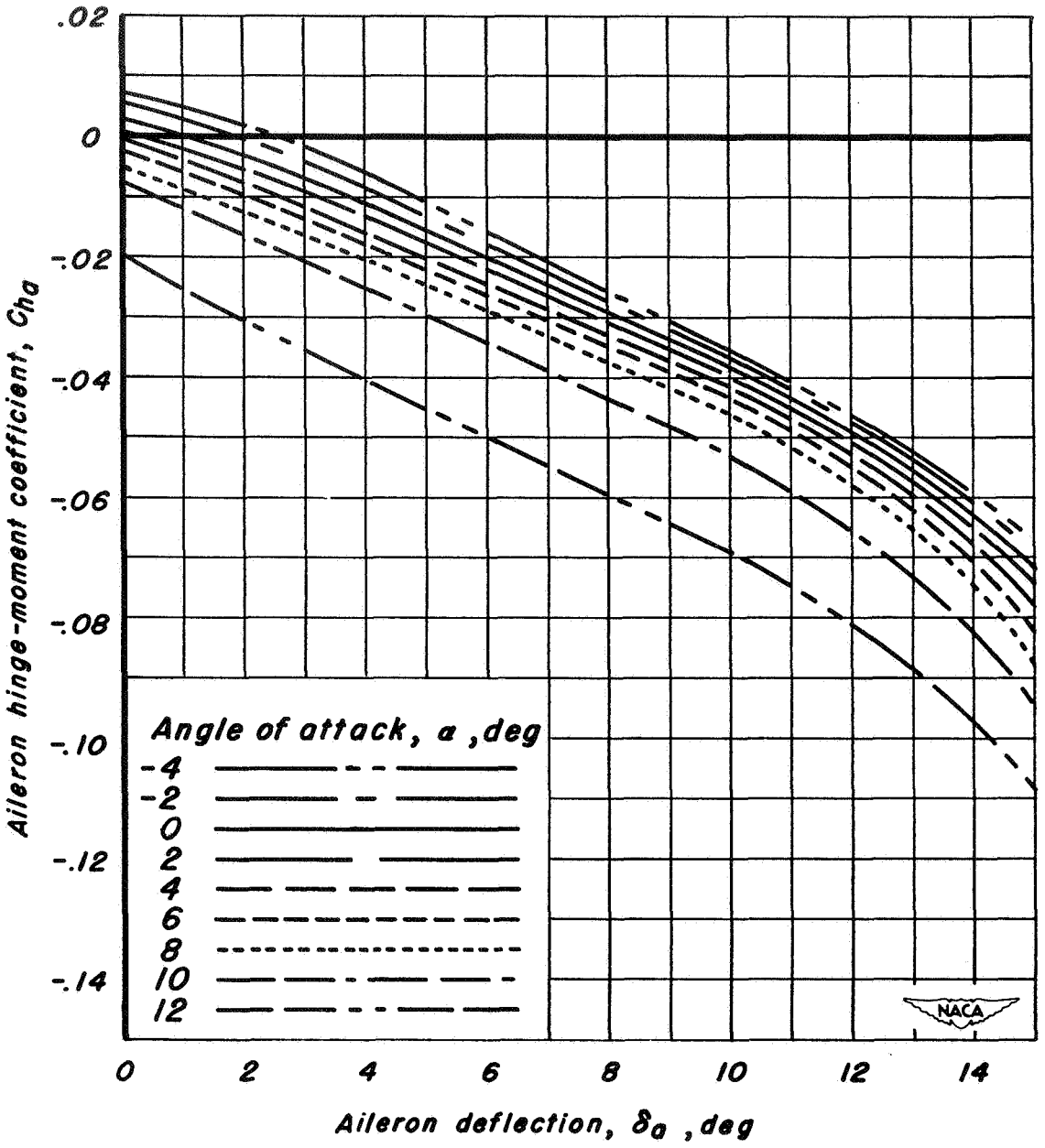

(a) M, 0.40.

Figure 12.- Variation of trailing-edge aileron hinge-moment coefficient with trailing-edge aileron deflection. Wing swept back.

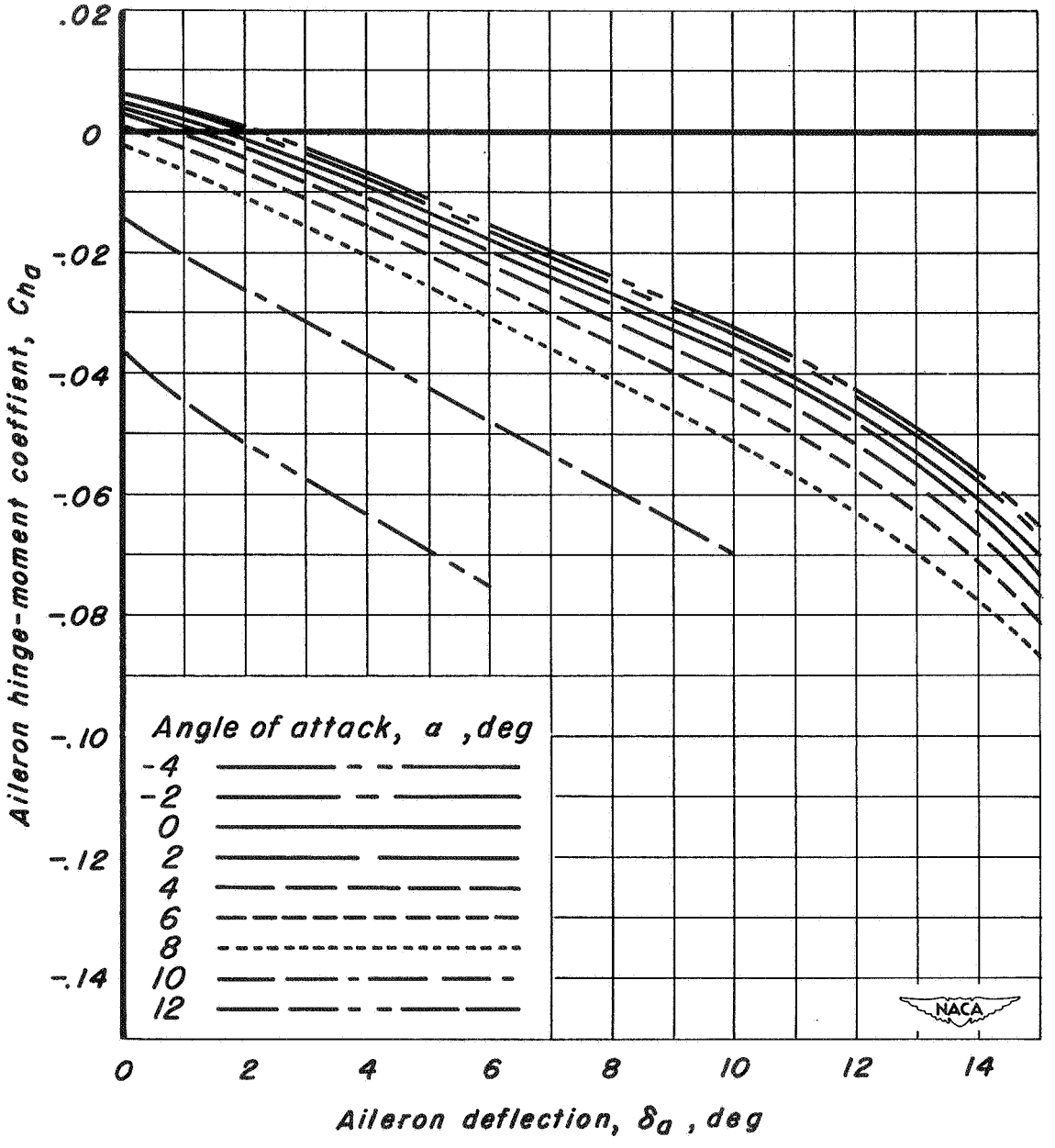

(b) M, 0.60.

Figure 12.— Continued.

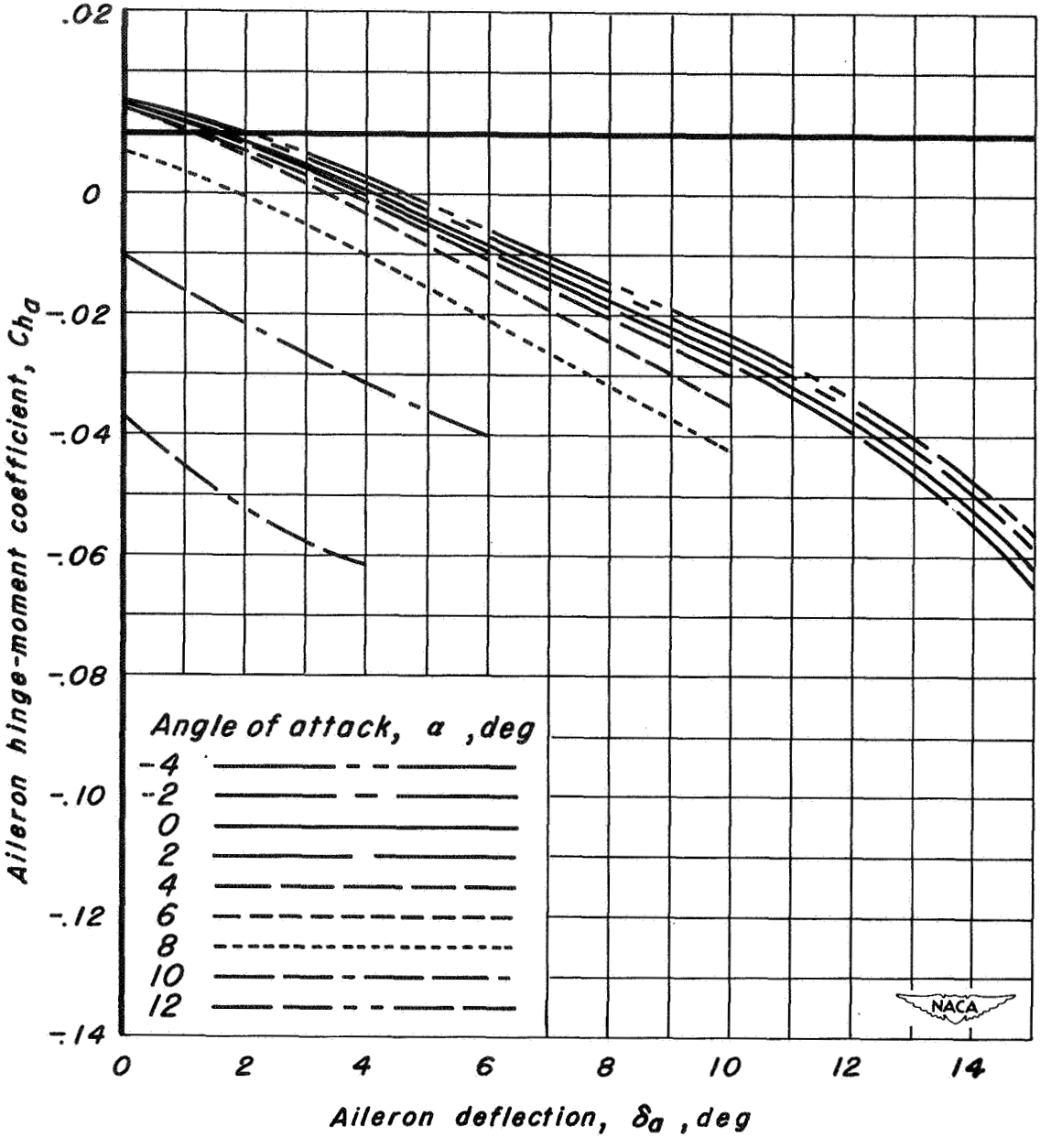

(c) M, 0.70.

Figure 12.- Continued.

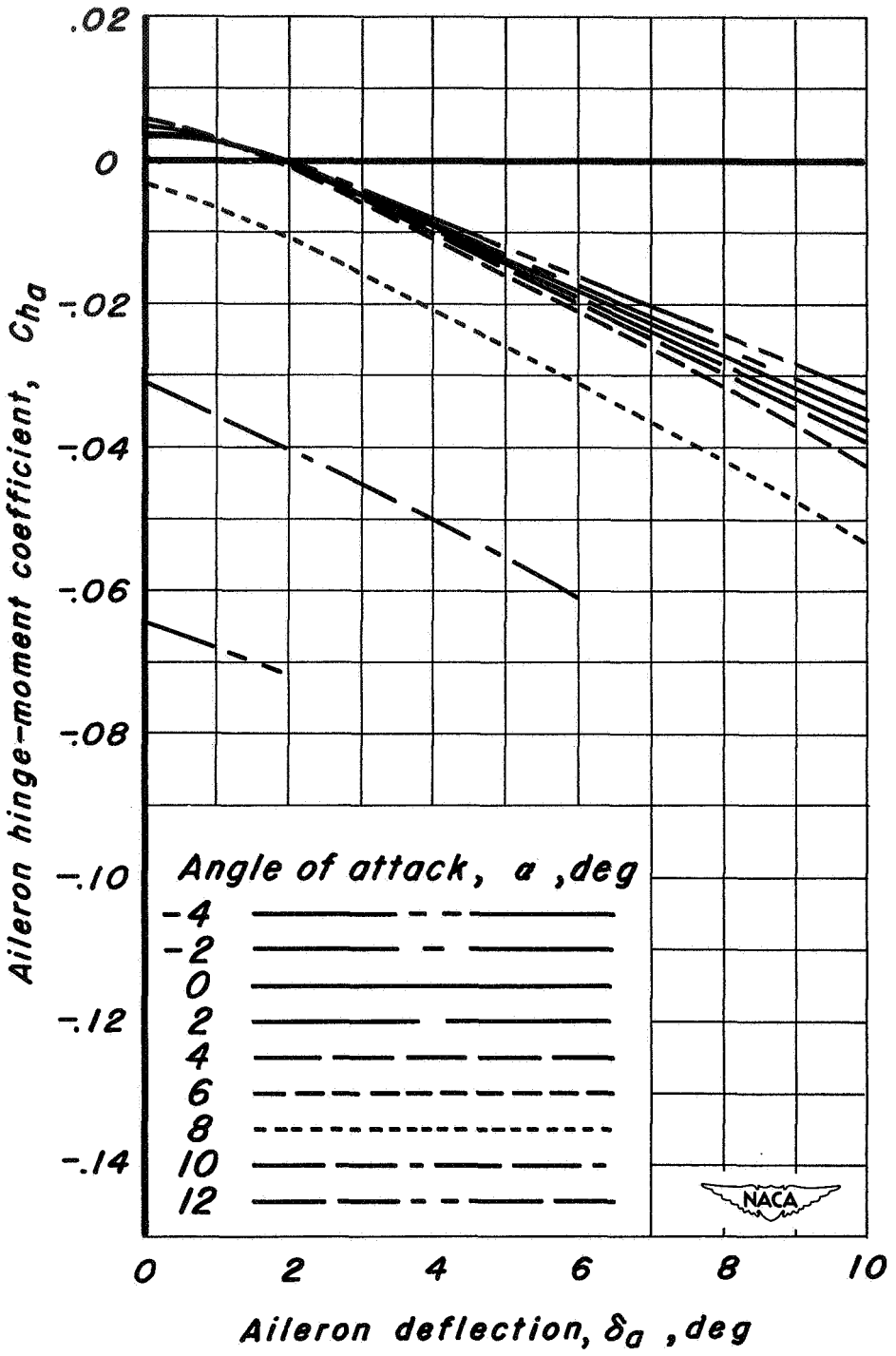

(d) M, 0.75.

Figure 12.—Continued.

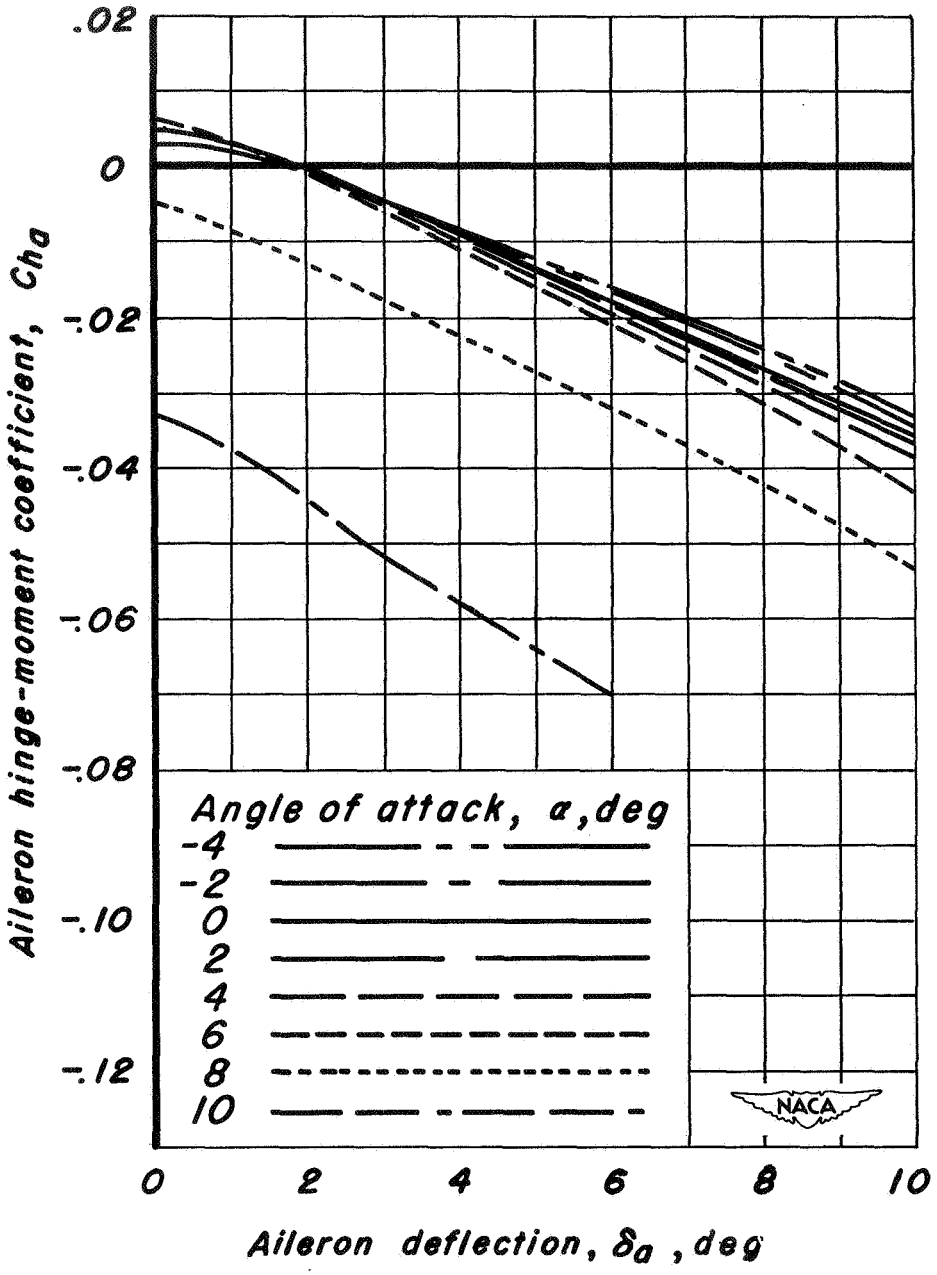

(e) M, 0.80.

Figure 12.- Continued.

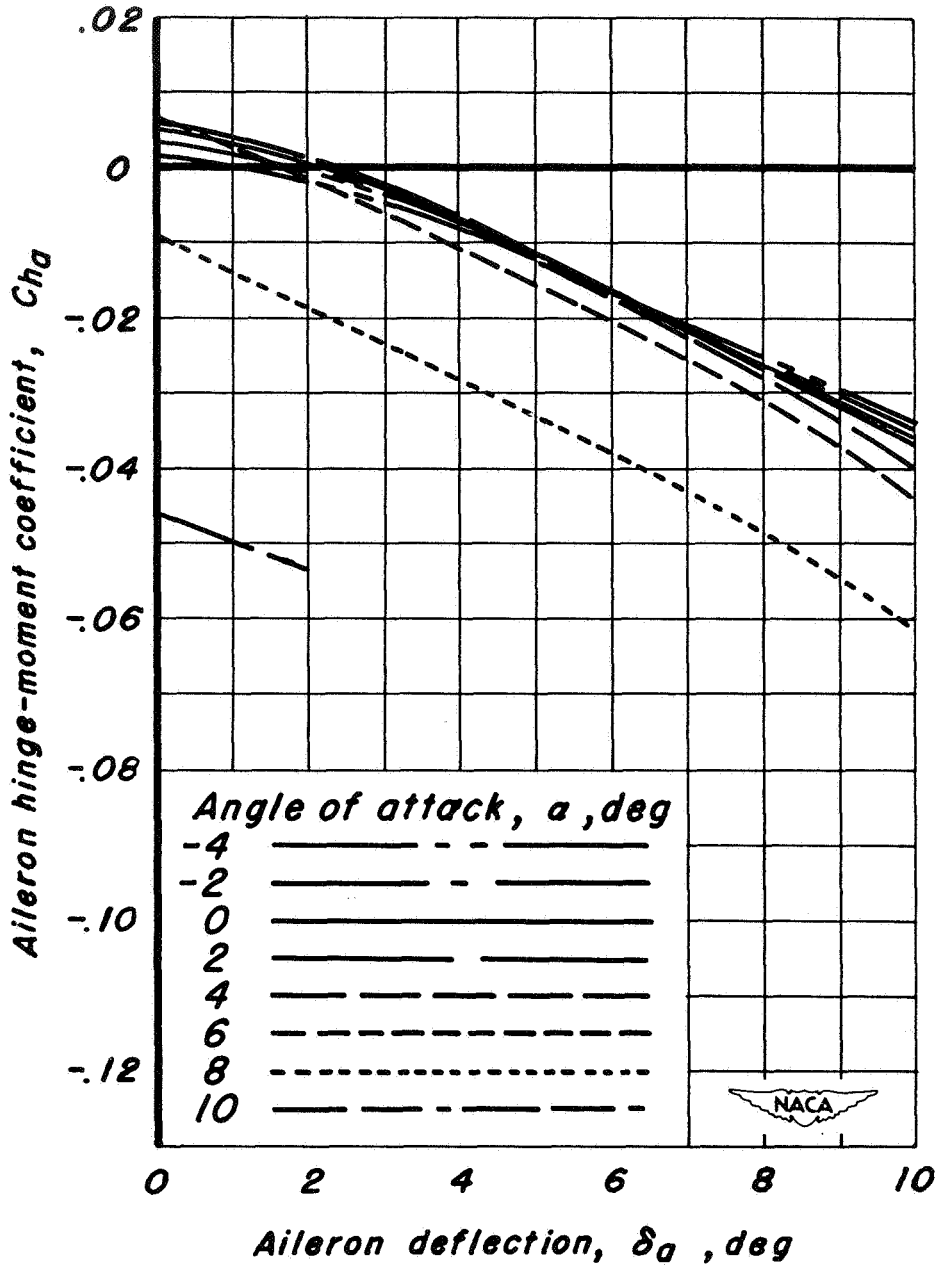

(f) M, 0.825.

Figure 12.- Continued.

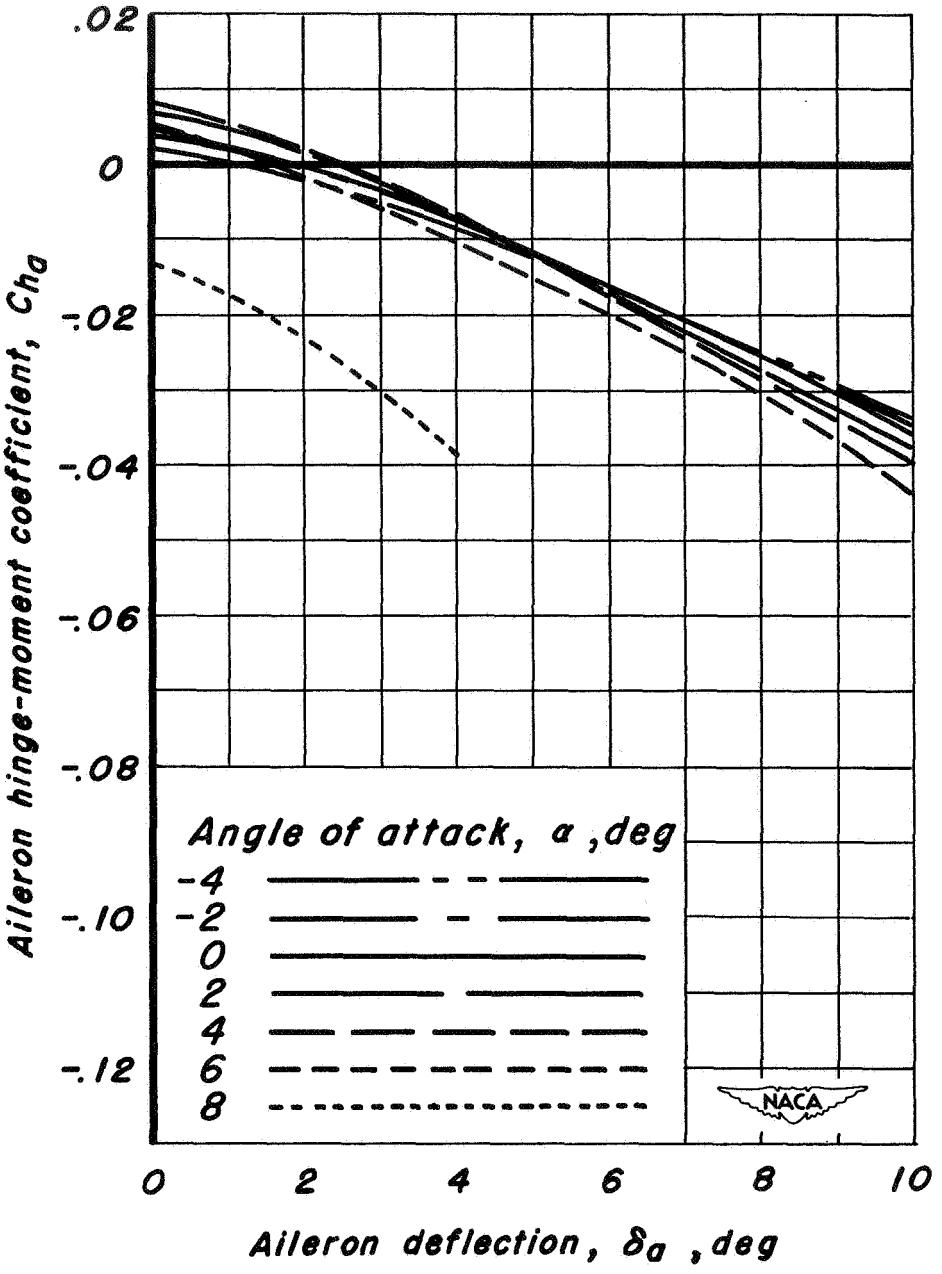

(g) M, 0.85.

Figure 12.- Continued.

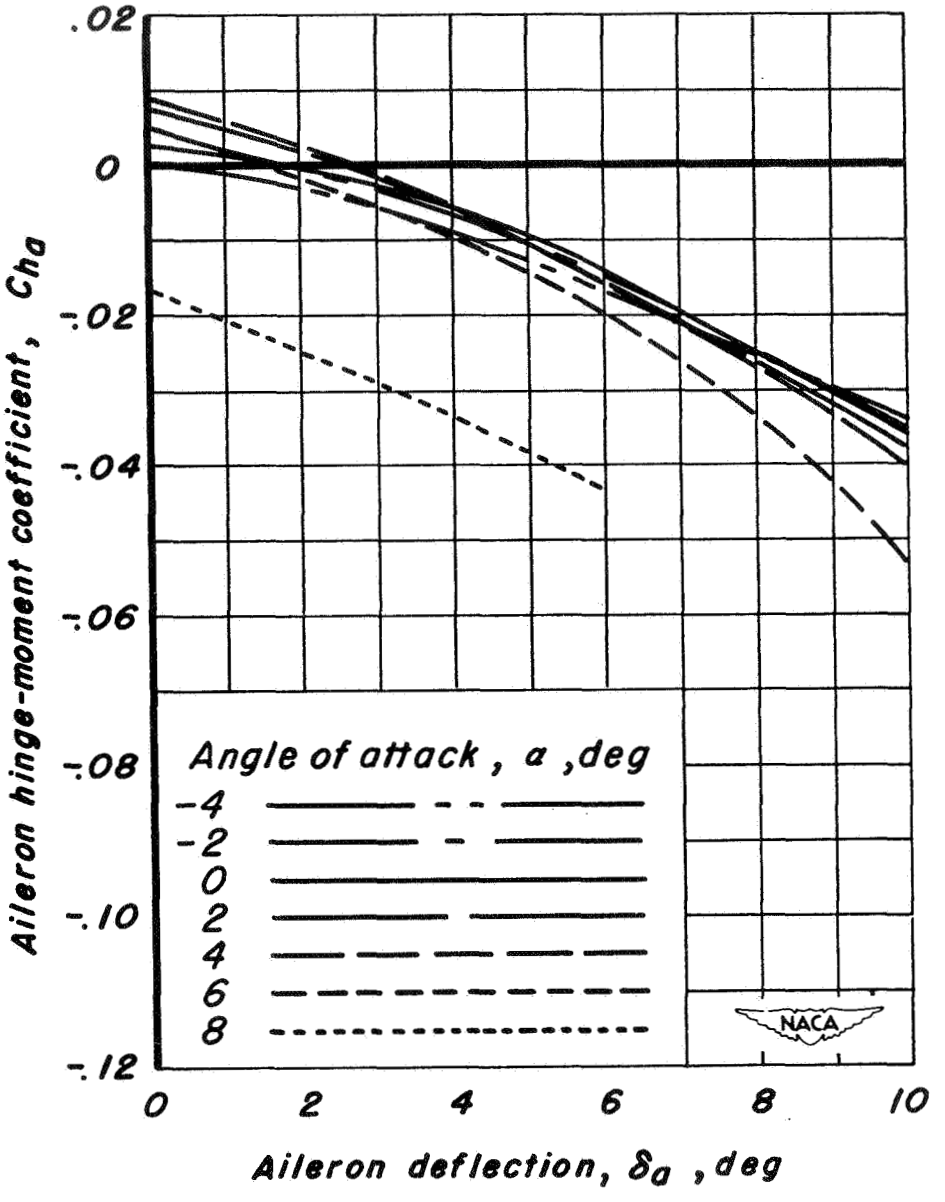

(h) M, 0.875.

Figure 12.- Continued.

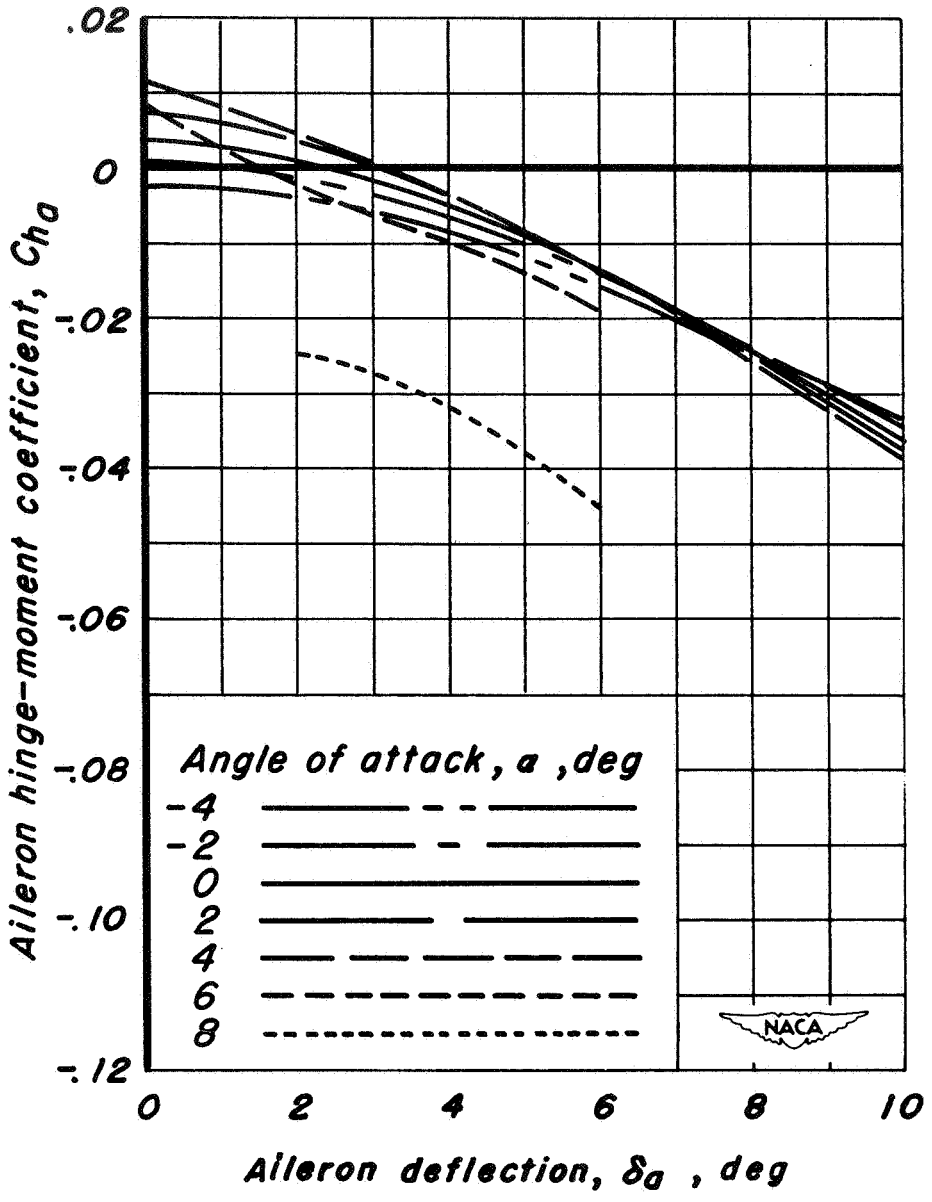

(i) M, 0.90.

Figure 12.- Continued.

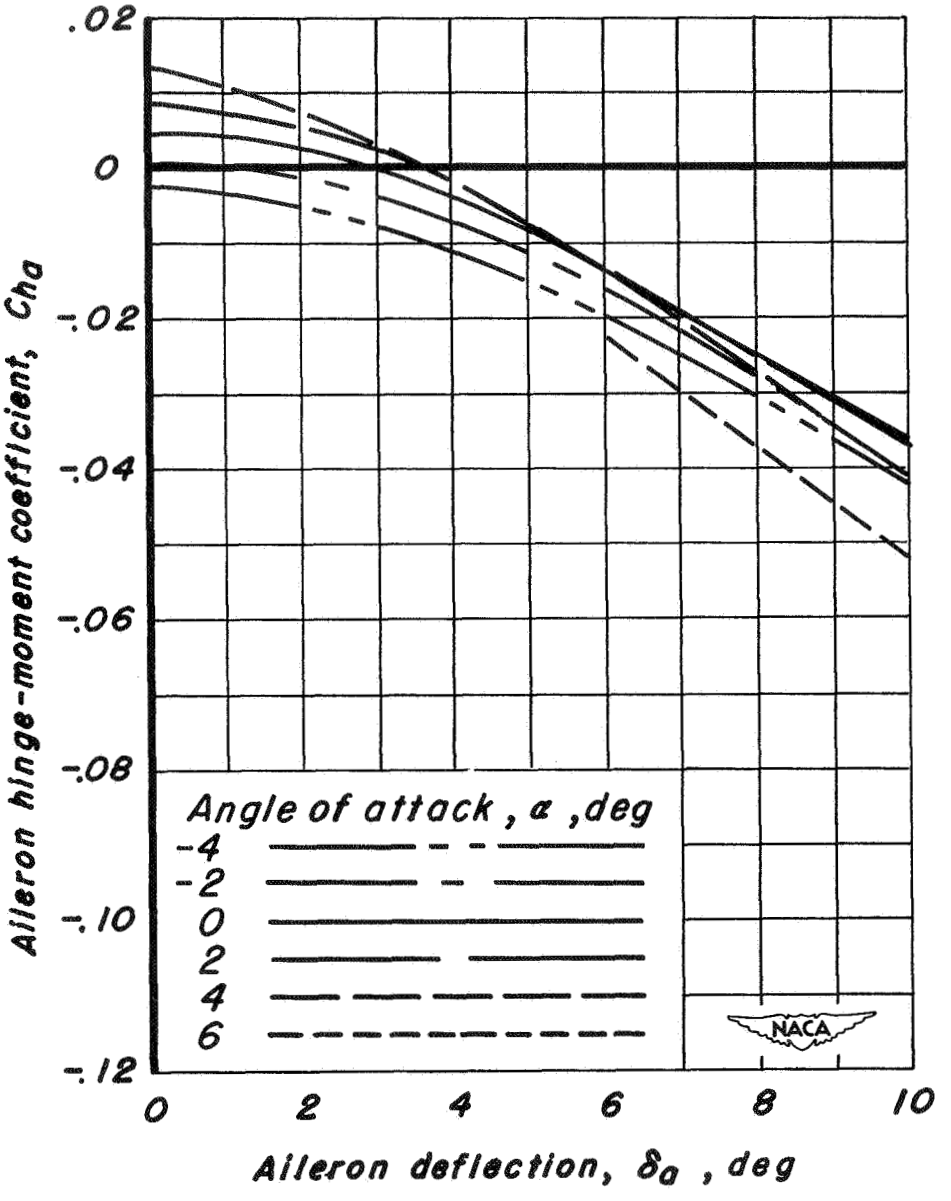

(j) M, 0.925.

Figure 12.- Concluded.